Accepted Manuscript

Synthesis and characterization of nitrile functionalized silver(I)-*N*-heterocyclic carbene complexes: DNA binding, cleavage studies, antibacterial properties and mosquitocidal activity against the dengue vector, *Aedes albopictus*

Patrick O. Asekunowo, Rosenani A. Haque, Mohd. R. Razali, Silas W. Avicor, Mustafa F.F. Wajidi

PII: S0223-5234(18)30272-1

DOI: 10.1016/j.ejmech.2018.03.029

Reference: EJMECH 10294

To appear in: *European Journal of Medicinal Chemistry*

Received Date: 23 January 2018

Revised Date: 28 February 2018

Accepted Date: 8 March 2018

Please cite this article as: P.O. Asekunowo, R.A. Haque, M.R. Razali, S.W. Avicor, M.F.F. Wajidi, Synthesis and characterization of nitrile functionalized silver(I)-*N*-heterocyclic carbene complexes: DNA binding, cleavage studies, antibacterial properties and mosquitocidal activity against the dengue vector, *Aedes albopictus*, *European Journal of Medicinal Chemistry* (2018), doi: 10.1016/j.ejmech.2018.03.029.

Graphical abstract

A new series of benzimidazolium based nitrile–functionalized Ag(I)–*N*-heterocyclic carbene complexes was developed by the deprotonation of the benzimidazolium salts and refluxing the benzimidazolium salts in the presence of a slight excess of Ag_2O. The most promising lead of this series, compound **8b**, were highly larvicidal and adversely affected the development of larvae into adults at the tested concentrations.

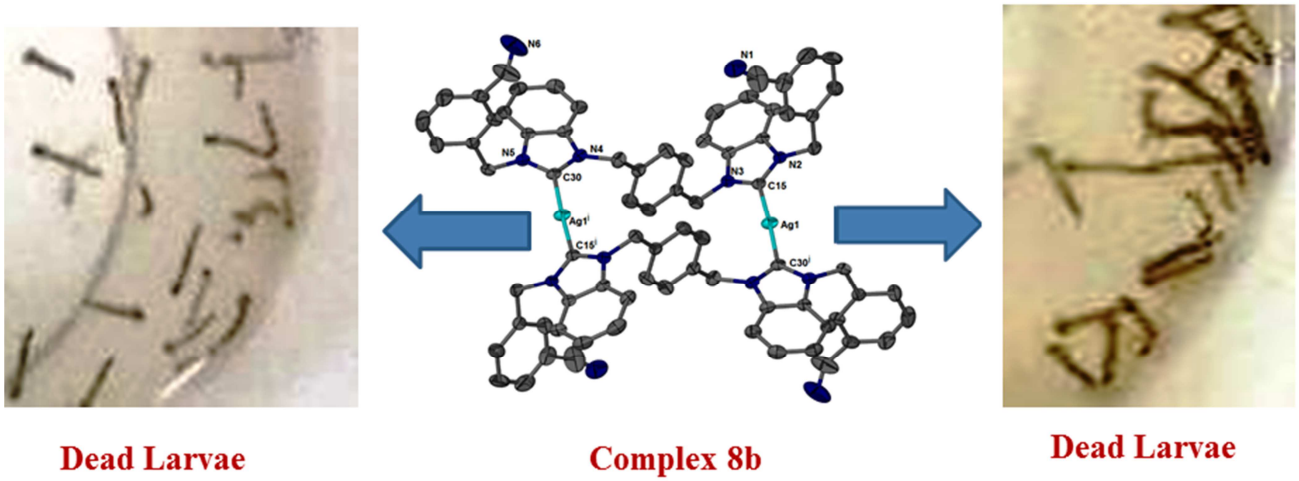

Synthesis and characterization of nitrile functionalized silver(I)-*N*-heterocyclic carbene complexes: DNA binding, cleavage studies, antibacterial properties and mosquitocidal activity against the dengue vector, *Aedes albopictus*

Patrick O. Asekunowo*[ab], Rosenani A. Haque [a], Mohd. R. Razali [a], Silas W. Avicor *[cd], Mustafa F.F. Wajidi [c]

[a]*School of Chemical Sciences, Universiti Sains Malaysia, 11800 USM, Penang, Malaysia*
[b]*Department of Chemical Sciences, Mountain Top University, KM 12, Lagos-Ibadan Express Way, Ogun State, Nigeria*
[c]*Molecular Entomology Research Group, School of Distance Education, Universiti Sains Malaysia, 11800 USM, Penang, Malaysia*
[d]*Entomology Division, Cocoa Research Institute of Ghana, P. O. Box 8, New Tafo-Akim, Ghana.*

**Corresponding email: poasekunowo@mtu.edu.ng*
**Corresponding email: wintuma@yahoo.co.uk*

ABSTRACT

A series of four benzimidazolium based nitrile–functionalized mononuclear–Ag(I)–*N*-heterocyclic carbene and binuclear–Ag(I)–*N*-heterocyclic carbene (Ag(I)–NHC) hexafluorophosphate complexes (**5b**–**8b**) were synthesized by reacting the corresponding hexafluorophosphate salts (**1b**–**4b**) with Ag_2O in acetonitrile, respectively. These compounds were characterized by ^{1}H NMR, ^{13}C NMR, IR, UV–visible spectroscopic techniques, elemental analyses and molar conductivity. Additionally, **8b** was structurally characterized by single crystal X-ray diffraction technique. Preliminary *in vitro* antibacterial evaluation was conducted for all the compounds against two standard bacteria; gram–positive (*Staphylococcus aureus*) and gram–negative (*Escherichia coli*) bacterial strains. Most of the Ag(I)–NHC complexes (**5b**–**8b**) showed moderate to good antibacterial activity with MIC values in the range of 12.5–100 μg/mL. Especially, compound **8b** exhibited promising anti–*Staphylococcus aureus* activity with a low MIC value (12.5 μg/mL). However, all the hexafluorophosphate salts (**1b**–**4b**) were inactive against the bacteria strains. The preliminary

interactive investigation revealed that the most active compound, **8b,** could effectively intercalate into DNA to form **8b**–DNA complex which shows a better binding ability for DNA (K_b = 3.627 x 10^6) than the complexes **5b**–**7b** (2.177 × 10^6, 8.672 × 10^5 and 6.665 × 10^5, respectively). Nuclease activity of the complexes on plasmid DNA and *Aedes albopictus* genomic DNA was time-dependent, although minimal. The complexes were larvicidal to the mosquito, with **5b**, **6b** and **8b** being highly active. Developmental progression from the larval to the adult stage was affected by the complexes, progressively being toxic to the insect's development with increasing concentration. These indicate the potential use of these complexes as control agents against bacteria and the dengue mosquito *Ae. albopictus.*

Keywords:
Aedes albopictus DNA; Ag–NHC complex; DNA binding; *N*–heterocyclic carbene; nuclease activity; X–ray diffraction.

1. Introduction

Nitrogen-containing heterocycles have been used as medicinal compounds for centuries, and form the basis for many common drugs such as Morphine (analgesic), Captopril (treatment of hypertension) and Vincristine (cancer chemotherapy). Benzimidazole and imidazole are frequently classified by medicinal chemists as privileged 'sub-structures' for drug dosing owing to the affinity they exhibit towards some enzymes and protein receptors. In the past few years, imidazole and its derivatives have received much attention as a result of their chemotherapeutic values. Imidazole analogue systems are present in a constituent of several important natural products, such as histidine, histamine, purine and nucleic acids [1].

(Benz)imidazoles, their derivatives and transition metal complexes have received considerable attention in coordination chemistry due to their well-documented biological activities [2 - 5]. It has been found that such complexes show better biological activities than the free ligands [6, 7]. However amongst these transition metals, Ag has shown low toxicity to humans and is present in the human body in very low concentrations (<2.3 μg/L), with its

absorption mostly through the lungs, skin, gastrointestinal tract and mucus membranes [8]. It is mainly found in the human body as silver protein complexes but has no physiological or biochemical role within the body [9]. It can be tolerated at high concentrations within the body, does not appear to be a cumulative poison and is eliminated from the body through the urine and faeces [8]. Recently, a number of researchers have reported promising biological activities of Ag(I)-NHC complexes as anticancer and antimicrobial agents [10-16]. However research on Ag(I)-NHC complexes as anti-malarial and anti-dengue agents remains scant. As a result of the foregoing, our research group continues to focus on providing Ag by incorporating Ag(I) to NHCs, and tuning both the electronic and steric properties to improve its stability in the body.

Dengue is the most important arthropod-borne viral infection of humans. Worldwide, an estimated 2.5 billion people are at risk of infection, approximately 975 million of whom live in urban areas in tropical and sub-tropical countries in Southeast Asia, the Pacific and the Americas [17]. Transmission also occurs in Africa and the Eastern Mediterranean, and rural communities are increasingly being affected. It is estimated that more than 50 million infections occur each year, including 500,000 hospitalizations for dengue haemorrhagic fever, mainly among children, with the fatality rate exceeding 5% in some areas [17-20].

The annual average number of dengue fever/dengue haemorrhagic fever (DF/DHF) cases reported to the World Health Organization (WHO) has increased dramatically in recent years. For the period 2000–2004, the annual average was 925,896 cases, almost double the figure of 479,848 cases that was reported for the period 1990–1999. In 2001, 69 countries reported dengue activity to the WHO and in 2002, the Region of the Americas alone reported more than 1 million cases [17-20]. To reduce or prevent dengue virus transmission, there is currently no alternative to vector control. Most endemic countries have a vector control component in their dengue control and prevention programmes but its delivery by public

health practitioners is frequently insufficient, ineffective or both. An obvious method for the control of mosquito-borne diseases is the use of insecticides, and many synthetic agents have been used in the field with considerable success. However, they also manifest undesirable effects, including toxicity to non-target organisms, giving rise to environmental and human health concerns [18].

Therefore, in an approach to find new compounds against this infective disease, this work aims to test a first series of air and moisture stable mononuclear and binuclear Ag(I)-*N*-functionalized NHC complexes against the major dengue vector, *Aedes albopictus*.

The interactive effects of the synthesized compounds on plasmid DNA and *Aedes albopictus* DNA were investigated in this study. This paper further explores the preliminary antibacterial activity of these complexes as well as their larvicidal and developmental inhibitory potentials on the mosquito to have a comparative insight into the bioactivity of these compounds.

2. Experimental

2.1. *Materials, Methods and Instruments*

All reactions were carried out under aerobic conditions unless otherwise specified. All Ag_2O reactions were carried out under the exclusion of light. The solvents were of analytical grade and used without further purification or drying. NMR spectra were recorded on a Bruker 500 MHz spectrometer at room temperature in DMSO-d_6. Chemical shifts (δ) were internally referenced to the residual solvent signals relative to tetramethylsilane. The values of chemical shifts are given in ppm and values for coupling constants (*J*) in Hz. Abbreviations for signal multiplicities are as follows: singlet (s), doublet (d), triplet (t), quartet (q), multiplet (m), and broad (br). FTIR spectra were recorded on Perkin-Elmer system 2000 FTIR spectrophotometer in the range 4000–400 cm^{-1}. Elemental analysis was carried out on a Perkin Elmer series II, 2400 microanalyzer. All electronic absorption spectra were taken in a quartz crystal cuvette with a PerkinElmer Lambda 35 spectrometer. Melting points were

measured using a Stuart Scientific SMP-1 (UK) instrument. Conductivity measurement was obtained from Jenway 470 Conductivity/TDS Meter, with conductivity resolution of 0.01µS-1mS* and accuracy of ±0.5% ±2 digits. Crystals were mounted on fine glass fibre or metal pin using viscous hydrocarbon oil. Data were collected on a Bruker-Smart ApexII-2009 CCD diffractometer, equipped with graphite monochromated Mo-Kα (λ = 0.71073 Å). Data collection temperatures were maintained at 100 K using open flow N_2 cryostreams. Integration was carried out by the program SAINT using the APEX II software [21]. The solutions were obtained by direct methods using SHELXS97, followed by successive refinements using full-matrix least-squares method against F^2 using SHELXL97 [22]. The X-seed program was used as graphical SHELX interface [23]. The crystal data and refinement details for complex **8b** are provided in Table S1. The higher R value is due to the disordered counter anions, PF6 (Table S1).

2.2. Synthesis of benzimidazolium salts

*2.2.1. Synthesis of 1-cyanopropyl-3-pentyl-benzimidazolium hexafluorophosphate (**1b**)*

N-cyanopropylbenzimidazole (0.70 g, 3.78 mmol) was added dropwise to a stirring solution of 1-bromopentane (0.57 g, 3.78 mmol) in dioxane (20 mL) and refluxed at 100^{o}C for 2 days. The solvent was removed under reduced pressure to obtain 1-cyanopropyl-3-pentylbenzimidazolium bromide (**1a**). The bromide salt was filtered and washed with fresh 1,4-dioxane and diethyl ether. The bromide salt was then reacted with a solution of KPF_6 (1.04 g, 5.67 mmol) in methanol (20 mL) and stirred for 3 h to precipitate a white solid (**1b)**. The precipitate formed was filtered, washed with distilled water (3 × 5 mL) to remove unreacted KPF_6, washed with diethyl ether and then dried at room temperature. Yield: 77.5%; m.p. 134-136^{o}C. ^{1}H NMR (500 MHz, DMSO-d_6, 298K, δ ppm): 0.89 (t, J = 7.0 Hz, 3H, CH_3); 1.32 (m, 2H, **CH$_2$**-CH_3); 1.95 (m, 2H, **CH$_2$**-CH_2-CH_3); 2.27 (m, 2H, N-CH_2-**CH$_2$**); 2.73 (t, J = 7.0 Hz, 2H, **CH$_2$**-CH_2-CN); 4.49 (t, J = 7.0 Hz, 2H, CH_2-CN); 4.63 (t, J = 7.0 Hz, 2H, N-**CH$_2$**-R); 4.70 (t, J = 7.0 Hz, 2H, N-**CH$_2$**-CH_2-CH_2-CN); 7.72 (m, 2H,

benzimidazolium-CH); 8.12 (m, 2H, benzimidazolium-CH); 9.99 (s, 1H, NC*H*N). $^{13}C\{^{1}H\}$ NMR (125 MHz, DMSO-d_6, 298K, δ ppm): 10.2 (CH_3); 23.8 (**CH_2**-CH_3); 30.9 (**CH_2**-CN); 40.0 (N-CH_2); 48.7 (N-**CH_2**-CH); 116.5 (C≡N); 118.3, 121.5, 127.1, 132.5 (benzimidazolium-C); 137.5 (benzimidazolium-C2′). FTIR (KBr disc) in cm^{-1}, ~ 3143 (C-H_{ar}); 2947 (C-H_{aliph}); 2249 (C≡N) 1432 (C=N). Anal. Calc. for $C_{16}H_{22}N_3F_6P$ (%): C, 47.88; H, 5.49; N, 10.47%. Found (%): C, 48.14; H, 5.62; N, 10.59. Molar conductance in DMF: 25.16 S cm^2 mol^{-1}

*2.2.2. Synthesis of 1-cyanopropyl-3-(3-cyanobenzyl)benzimidazolium hexafluorophosphate (**2b**)*

A mixture of 3-bromomethyl benzonitrile (0.20 g, 1 mmol) and *N*-cyanopropylbenzimidazole (0.185 g, 1 mmol) were stirred in dioxane (20 mL) at 100°C for 2 days. The solvent was removed under reduced pressure, and the product was then washed with 1,4 dioxane and diethyl ether. The bromide salt **2a** thus obtained was recrystallized from acetonitrile/methanol (1:5 v/v). Salt **2a** was directly converted into its hexafluorophosphate counterpart (**2b**) by metathesis reaction using KPF_6 (0.28 g, 1.5 mmol) in methanol (20 mL). The resultant mixture was stirred for 3 h and was allowed to stand overnight. The pale yellow precipitate was filtered under reduced pressure, washed with distilled water (3 × 5 mL) to remove unreacted KPF_6, and air dried. Yield 67.7 %; m.p. 144–146°C. ^{1}H NMR (500 MHz, DMSO-d_6): δ 2.36 (m, 2H, **CH_2**-CH_2-CN); 2.79 (t, *J* = 7.0 Hz, 2H, CH_2-CN); 4.68 (t, *J* = 7.0 Hz, 2H, N-**CH_2**-CH_2-CH_2-CN), 5.93 (s, 2H, N-**CH_2**); 7.66 (m, 3H, benzimidazolium-CH), 7.85 (d, *J* = 8.0 Hz, 1H, benzimidazolium-CH); 7.96 (d, *J* = 8.0 Hz, 2H, benzonitrile-CH); 8.07 (s, 1H, Benzonitrile-CH), 8.20 (d, *J* = 8.0 Hz, 1H, Benzonitrile-CH), 10.15 (s, 1H, NC*H*N). $^{13}C\{^{1}H\}$NMR (125 MHz, DMSO-d_6): δ 13.8 (CH_2-CH_2-CN), 32.3 (CH_2-CN), 48.9 (N-CH_2-R) 66.3 (CH_2-benzonitrile), 110.9 (C≡N-nitrile), 113.8, 116.9, (benzimidazole-C), 133.0, 134.0, 135.9, (Benzonitrile-C), 143.1 (benzimidazolium C2′). FT-IR (KBr disc) cm^{-1}: ~ 3033 (C-H_{ar}); 2926 (C-H_{aliph}); 2230 (C≡N) 1568 (C=N). Anal. Calc. for $C_{19}H_{17}N_4F_6P$(%): C, 51.12;

H, 3.81; N, 12.56. Found(%): C, 51.34; H, 3.97; N, 12.79. Molar conductance in DMF: 24.76 S cm^2 mol^{-1}

*2.2.3. Synthesis of 1,3-bis(3-cyanobenzyl)benzimidazolium hexafluorophosphate (**3b**)*

A mixture of 3-bromomethyl benzonitrile (0.50 g, 2.55 mmol) and *N*-cyanobenzylbenzimidazole (0.60 g, 2.55 mmol) were stirred in dioxane (20 mL) at 100°C for 2 days. The solvent was removed under reduced pressure, and the product was then washed with 1,4 dioxane and diethyl ether. Salt **3a** was directly converted into its hexafluorophosphate counterpart (**3b**) by metathesis reaction using KPF_6 (0.28 g, 1.5 mmol) in methanol (20 mL). The resultant mixture was stirred for 3 h and was allowed to stand overnight. The pale yellow precipitate was filtered under reduced pressure, washed with distilled water (3 × 5 mL) to remove unreacted KPF_6, and air dried. Yield 67.7 %; m.p. 154–156°C. ^{1}H NMR (500 MHz, DMSO-d_6): 5.93 (s, 4H, N-$\mathbf{CH_2}$); 7.66 (m, 4H, benzimidazolium-CH), 7.91 (d, *J* = 8.0 Hz, 2H, benzonitrile-CH); 8.01 (m, 4H, benzonitrile-CH); 8.12 (s, 2H, benzonitrile-CH), 10.21 (s, 1H, NC*H*N). ^{13}C{^{1}H}NMR (125 MHz, DMSO-d_6): δ 13.8 (CH_2-CH_2-CN), 32.3 (CH_2-CN), 46.9 (N-CH_2-R) 62.3 (CH_2-benzonitrile), 110.9 (C≡N-nitrile), 113.8, 116.9, (benzimidazole-C), 133.0, 134.0, 135.9, (Benzonitrile-C), 143.5 (benzimidazolium C2′). FT-IR (KBr disc) cm^{-1}: ~ 3130 (C-H_{ar}); 2960 (C-H_{aliph}); 2229 (C≡N); 1562 (C=N). Anal. Calc. for $C_{23}H_{17}N_4F_6P$(%): C, 55.87; H, 3.44; N, 11.34. Found(%): C, 56.14; H, 3.67; N, 11.51. Molar conductance in DMF: 26.76 S cm^2 mol^{-1}.

*2.2.4. Synthesis of 1,4-bis(3-cyanobenzylbenzimidazol-1-ylmethyl)benzene hexafluorophosphate (**4b**)*

A mixture of benzimidazole (1.00 g, 8.46 mmol) and KOH (1.43 g, 12.69 mmol) in DMSO (20 mL) was stirred for 1 h at room temperature. 3-bromomethyl benzonitrile (1.66 g, 8.46 mmol) was added portionwise and the mixture was stirred at room temperature for 2 h. After 2 h, the mixture was poured into 200-300 mL of water and extracted with chloroform (3 × 30

mL). The extract was filtered twice through four plies of Whatman filter paper in order to dry the extract. The desired compound was finally evaporated under reduced pressure and a thick yellow oil was obtained. The compound formed, *N*-cyanobenzylbenzimidazole (1.0 g, 4.30 mmol) was added dropwise to a stirring solution of 1,4-bis(bromomethyl)benzene (0.57 g, 2.15 mmol) in dioxane (20 mL) and refluxed for 3 days. The solvent was removed under reduced pressure to give 1,4-bis(3-cyanobenzyl-1-ylmethyl)benzene dibromide and washed in dioxane and diethyl ether which was then reacted with a solution of KPF_6 (0.80 g, 4.35 mmol) in methanol (20 mL). The mixture was stirred at room temperature for 3 h and allowed to stand overnight. The solvent was removed under reduced pressure and the resultant brown powder was washed with distilled water (3 × 5 mL) to remove unreacted KPF_6, and air dried. The powder was recrystallized in a solution of acetonitrile/methanol to obtain a crystalline solid. Yield: 69%; mp: 187-189^{o}C. ^{1}H NMR (500 MHz, DMSO-d_6): 5.80 (s, 4H, N-**CH_2**); 5.95 (s, 4H, N-**CH_2**-benzonitrile); 7.48 (s, 4H, 4 × Ar-CH), 7.66 (m, 8H, benzimidazolium-CH), 7.91 (d, *J* = 8.0 Hz, 2H, benzonitrile-CH); 8.01 (m, 4H, benzonitrile-CH); 8.12 (s, 2H, benzonitrile-CH), 10.15 (s, 1H, NC*H*N). ^{13}C{^{1}H}NMR (125 MHz, DMSO-d_6): δ 13.8 (CH_2-CH_2-CN), 32.3 (CH_2-CN), 46.9 (N-CH_2-R) 62.3 (CH_2-benzonitrile), 110.9 (C≡N-nitrile), 113.8, 116.9, (benzimidazole-C), 133.0, 134.0, 135.9, (Benzonitrile-C), 143.1 (benzimidazolium C2′). FT-IR (KBr disc) cm^{-1}: ~ 3015 (C-H_{ar}); 2920 (C-H_{aliph}); 2232 (C≡N); 1556 (C=N). Anal. Calc. for $C_{38}H_{30}N_6F_{12}P_2$(%): C, 47.12; H, 3.93; N, 10.99. Found(%) : C, 47.34; H, 4.17; N, 11.21. Molar conductance in DMF: 52.67 S cm^2 mol^{-1}.

2.3. Synthesis of Ag(I)-NHC complexes

2.3.1. *Synthesis of 1-cyanopropyl-3-pentyl-benzimidazolium-silver(I) hexafluorophosphate (**5b**)*

Ag_2O (0.80 g, 3.45 mmol) was added to a solution of 1-cyanopropyl-3-pentyl-benzimidazolium hexafluorophosphate (**1b**) (1.38 g, 3.45 mmol) with molecular sieves (3 Å beads) in acetonitrile (40 mL), protected from light and stirred for 24 h under nitrogen at

50°C. A clear solution with some black suspension was obtained. The solution was filtered through Celite®, evaporated under reduced pressure and the solid was poured into water (50 mL). The resulting white powder was collected by filtration and the solid was washed three times with distilled water. Recrystallization of the powder from acetonitrile yielded a crystalline solid (53%); m.p: 224-226°C. ^{1}H NMR (500 MHz, DMSO-d_6, 298K, δ ppm): 0.87 (t, J = 7.0 Hz, 6H, CH_3); 1.33 (m, 8H, **CH_2-CH_2**-CH_3); 1.92 (m, 4H, N-CH_2-**CH_2**); 2.27 (t, J = 7.0 Hz, 4H, **CH_2**-CH_2-CN); 2.68 (t, J = 7.0 Hz, 4H, CH_2-CN); 4.58 (t, J = 7.0 Hz, 4H, N-**CH_2**-R); 4.68 (t, J = 7.0 Hz, 2H, N-**CH_2**-CH_2-CH_2-CN); 7.50 (m, 2H, benzimidazolium-CH); 7.91 (m, 2H, benzimidazolium-CH). ^{13}C{^{1}H} NMR (125 MHz, DMSO-d_6, 298K, δ ppm): 10.2 (CH_3); 23.8 (**CH_2**-CH_3); 30.9 (**CH_2**-CN); 40.0 (N-CH_2); 48.7 (N-**CH_2**-CH); 116.5 (C≡N); 118.3, 121.5, 127.1, 132.5 (benzimidazolium-C); 188.3 (benzimidazolium C2′-Ag). FTIR (KBr disc) in cm^{-1}, ~ 3069 (C-H_{ar}); 2925 (C-H_{aliph}); 2249 (C≡N) 1406 (C=N). Anal. Calc. for $C_{32}H_{42}N_6AgF_6P$ (%): C, 50.33; H, 5.50; N, 11.01. Found (%): C, 50.61; H, 5.72; N, 11.29. Molar conductance in DMF: 27.76 S cm^2 mol^{-1}

*2.3.2. Synthesis of 1-cyanopropyl-3-(3-cyanobenzyl)benzimidazolium-silver(I) hexafluorophosphate (**6b**)*

Complex **6b** was prepared by adopting a procedure similar to that used for complex **5b** except that **1b** was replaced by **2b** (1.00 g, 2.24 mmol) and Ag_2O (0.52 g, 2.24 mmol). Complex 6b was isolated as a white powder. Yield: 71%; mp: 230-232°C. ^{1}H NMR (500 MHz, DMSO-d_6): δ 2.23 (m, 4H, **CH_2**-CH_2-CN); 2.62 (t, J = 7.0 Hz, 4H, CH_2-CN); 4.66 (t, J = 7.0 Hz, 4H, N-**CH_2**-CH_2-CH_2-CN); 5.82 (s, 4H, N-**CH_2**); 7.50 (m, 3H, benzimidazolium-CH), 7.64 (d, J = 8.0 Hz, 1H, benzimidazolium-CH); 7.71 (d, J = 8.0 Hz, 2H, benzonitrile-CH); 7.81 (s, 1H, Benzonitrile-CH), 7.93 (d, J = 8.0 Hz, 1H, Benzonitrile-CH). ^{13}C{^{1}H}NMR (125 MHz, DMSO-d_6): δ 13.8 (CH_2-CH_2-CN), 32.3 (CH_2-CN), 48.9 (N-CH_2-R) 66.3 (CH_2-benzonitrile), 110.9 (C≡N-nitrile), 113.8, 116.9, (benzimidazole-C), 133.0, 134.0, 135.9, (Benzonitrile-C), 189.2, 190.4 (benzimidazolium C2′-Ag). FT-IR (KBr disc)

cm^{-1}: ~ 3060 (C-H_{ar}); 2926 (C-H_{aliph}); 2230 (C≡N) 1479 (C=N). Anal. Calc. for $C_{38}H_{32}N_8AgF_6P$(%): C, 53.46; H, 3.75; N, 13.13. Found(%): C, 53.84; H, 3.87; N, 13.49. Molar conductance in DMF: 25.44 S cm^2 mol^{-1}.

*2.3.3. Synthesis of 1,3-bis(3-cyanobenzyl)benzimidazolium-silver(I) hexafluorophosphate (**7b**)*

Complex **7b** was prepared by adopting a procedure similar to that used for complex **5b** except that **1b** was replaced by **3b** (1.00 g, 2.24 mmol) and Ag_2O (0.52 g, 2.24 mmol). Complex **7b** was isolated as a white powder. Yield: 62%; mp: 239-241^oC. ^1H NMR (500 MHz, DMSO-d_6): 5.88 (s, 8H, N-**CH_2**); 7.44(m, 8H, benzimidazolium-CH), 7.61 (d, J = 8.0 Hz, 4H, benzonitrile-CH); 7.72 (m, 8H, benzonitrile-CH); 7.82 (s, 2H, benzonitrile-CH). $^{13}C\{^1H\}$NMR (125 MHz, DMSO-d_6): δ 12.8 (CH_2-CH_2-CN), 31.3 (CH_2-CN), 44.9 (N-CH_2-R) 61.3 (CH_2-benzonitrile), 110.9 (C≡N-nitrile), 113.8, 116.9, (benzimidazole-C), 133.0, 134.0, 135.9, (Benzonitrile-C), 190.8 (benzimidazolium C2′-Ag). FT-IR (KBr disc) cm^{-1}: ~ 3069 (C-H_{ar}); 2956 (C-H_{aliph}); 2229 (C≡N); 1459 (C=N). Anal. Calc. for $C_{46}H_{32}N_8AgF_6P$(%): C, 58.17; H, 3.37; N, 11.80. Found(%): C, 58.29; H, 3.67; N, 11.91. Molar conductance in DMF: 27.76 S cm^2 mol^{-1}.

*2.3.4. Synthesis of 1,4-bis(3-cyanobenzylbenzimidazol-1-ylmethyl)benzene silver(I) hexafluorophosphate (**8b**)*

A mixture of the salt **4b** (267 mg, 0.46 mmol) and Ag_2O (105 mg, 0.46 mmol) in acetonitrile (40 mL) was heated at 50 °C for 2 days with molecular sieves (3 Å beads) in acetonitrile (40 mL) and the mixture was protected from light. A clear solution with black suspension was obtained. The mixture was filtered and concentrated under reduced pressure. Recrystallization of the residue from acetonitrile yielded a grey powder (63%). Crystals suitable for X-ray diffraction studies were grown by layering a concentrated solution of the complex in acetonitrile with neat diethyl ether. mp: 268-270^oC. ^1H NMR (500 MHz, DMSO-d_6): 5.71 (s, 8H, N-**CH_2**); 5.87 (s, 8H, N-**CH_2**-benzonitrile); 7.28 (s, 8H, 4 × Ar-CH), 7.45

(m, 16H, benzimidazolium-CH), 7.74 (d, *J* = 8.0 Hz, 4H, benzonitrile-CH); 7.88 (m, 8H, benzonitrile-CH); 8.01 (s, 4H, benzonitrile-CH), $^{13}C\{^{1}H\}$NMR (125 MHz, DMSO-d_6): δ 13.2 (CH_2-CH_2-CN), 31.7 (CH_2-CN), 46.1 (N-CH_2-R) 61.5 (CH_2-benzonitrile), 110.9 (C≡N-nitrile), 112.2, 116.3, (benzimidazole-C), 131.0, 132.5, 134.2, (Benzonitrile-C), 188.9 (benzimidazolium C2′-Ag). FT-IR (KBr disc) cm^{-1}: ~ 3005 (C-H_{ar}); 2920 (C-H_{aliph}); 2232 (C≡N); 1455 (C=N). Anal. Calc. for $C_{76}H_{56}N_{12}Ag_2F_{12}P_2$(%): C, 55.54; H, 3.41; N, 10.23. Found(%): C, 55.87; H, 3.64; N, 10.51. Molar conductance in DMF: 59.25 S cm^2 mol^{-1}.

2.4. Biological Evaluation

2.4.1. Antibacterial studies

The antibacterial activities of the compounds were investigated against *Escherichia coli* and *Staphylococcus aureus*. Stock solutions of all the compounds were prepared using DMSO. Antibacterial tests were performed using the Kirby-Bauer disc diffusion method [24]. Single colonies of *E. coli* and *S. aureus* from fresh culture agar plates were respectively cultured in 5 mL of Luria-Bertani (LB) broth solution (Tryptone10 g, yeast extract 5 g, NaCl 10 g/L), and incubated overnight at 37°C. The turbidity of each culture was adjusted by comparing it to 0.5 McFarland standards, which is equal to 1.58×10^8 CFU/mL or 0.5 ($O.D_{600}$ reading). Single colonies were suspended in the Nutrient broth with incubation over a period of 2–5 h until an appropriate optical density (OD = 0.6–0.8) at 600 nm was achieved. Using sterile cotton buds, each bacterial lawn culture was spread uniformly on different agar plates before placing the sterile antimicrobial assay discs (5 mm) on the plate. Four discs were placed on the agar plate and 20 µL of the compounds and controls were loaded on the discs with concentrations at 200, 100, 50 and 25 µg/mL. The plates were incubated at 37°C for 24 h, after which the zones of clearance were measured as the difference between the diameter of the ring (inhibition zone and disc) and diameter of the disc. Diameters of the zones were measured with a Hi Antibiotic Zone Scale (PW 297-3NO, HiMedia Laboratories). The test

was performed three times for each sample and the diameter of inhibition zone was expressed as mean inhibition zone (mm) ± S.D of the three replicates. The effectiveness of these compounds in relation to their inhibition zones was compared to two positive controls; silver nitrate based on its established antimicrobial properties [25] and ciprofloxacin. Silver nitrate was also used to compare the activities of the Ag^+ from the complexes and the free Ag^+ that may be present, so as to eliminate the possibility that the observed activities of the complexes are not due to the free Ag^+ in solution. The minimum inhibitory concentration (MIC) of each compound was determined based on the lowest concentration of the compounds that inhibited the growth of bacteria using the broth dilution method [26]. Single colonies of *S. aureus*, and *E. coli* were isolated from agar plates and grown in 5.0 mL of LB broth. The solutions were incubated at 37°C and shaken at 180 rpm overnight to yield bacteria solutions. Stock solutions (50 mg/mL) of the compounds were prepared by dissolving each in DMSO. From each stock solution, the compounds, $AgNO_3$ and ciprofloxacin were dissolved in the broth culture and used to prepare serial dilutions of 200, 100, 50, 25, 12.5 and 6.25 µg/mL. Bacteria growth was noted by turbidity of the solution in the tubes and MIC was determined by the lowest concentration of the compounds that prevented visible growth. For the viable cell count method, the concentrations of the tested compounds were also 200, 100, 50, 25, 12.5 and 6.25 µg/mL. The bacterial strain was inoculated into the nutrient broth and was incubated for 16 h at 37°C. The stock was serially diluted to obtain 10^5 CFU/mL. About 60 µL of bacterial suspension was transferred into 3 mL of nutrient broth followed by 30 µL of sample suspension. The incubation was carried out for 5 h at 37°C and 50 µL of culture was uniformly spread on the nutrient agar which was incubated at 37°C for 24 h**.** The MIC was determined based on the lowest concentration of the silver samples that inhibited the growth of bacterial strain. For growth inhibitory concentrations, the presence of viable

microorganisms was tested and the lowest concentration causing bactericidal effect was reported as minimum bactericidal concentration (MBC).

2.4.2. Larval culture

Insecticide susceptible *Ae. albopictus* larvae from the Vector Control Research Unit (VCRU) of the School of Biological Sciences, Universiti Sains Malaysia were used for the study. The larvae were reared on a 2:1:1:1 powdered mixture of cat biscuits (Friskies), beef liver, yeast and powdered milk [27]. Larval breeding and experimental conditions were maintained at 26 ±2 ºC, 75±5 % relative humidity and 12 h : 12 h (light : dark) photoperiod. .

2.4.3. Larvicidal activity

Stock solutions (100 mg/mL) of the test compounds were prepared in DMSO and test concentrations of 400, 200, 100, 50, 25, 5 and 1 ppm were prepared from the stock solutions in distilled water to a final total volume of 100 mL for the bioactivity tests.

Fourth instar larvae (25) of *Ae. albopictus* were introduced into paper cups containing the test concentrations according to the WHO protocol [28]. Larval mortality was recorded after 24 h. Four replicates were performed for each concentration.

2.4.4. Bioactivity of test compounds on developmental progression of Ae. albopictus

Biological activity of the test chemicals on the developmental progression of larvae into pupae and adults were determined by introducing cohorts of fourth instar larvae (25) into paper cups containing 25, 5 and 1 ppm of the test compounds [28] and monitored for 6 days. DMSO was used as the control.

2.4.5. Statistical analysis

The lethal concentrations for 50 % (LC_{50}) and 90 % (LC_{90}) of the larvae and their respective 95 % confidence intervals (CI) in the larvicidal assay were computed using Qcal [29]. LCs with overlapping 95% CL were considered not significantly different [30, 31]. Bioactivity data from the developmental stages were arc sine transformed and analyzed using the one-

way analysis of variance followed by mean separation with Tukey HSD using IBM SPSS ver. 20. The formula of Abbott [32] was used to correct natural mortality prior to analysis.

2.5. DNA experiments

2.5.1. *DNA binding analysis using Absorption spectral method*

Aedes albopictus-DNA (*Aa*-DNA) extraction:

Aedes albopictus DNA (*Aa*-DNA) was extracted from virgin individual adult females (3 days old) for DNA binding activity using DNeasy® Blood and Tissue Kit (Qiagen®) according to the manufacturer's instruction. DNA extracted from individual female mosquitoes were pooled and used for the binding study.

The *Aa*-DNA was dissolved in buffer solution (10 mM phosphate buffer, 50 mM NaCl, pH 7.4) as a stock solution, which was stored at 4 ^{o}C for 24 h to reach homogeneous phase and used within three days. The *Aa*-DNA concentrations were determined by spectroscopy using the following extinction coefficients at 260 nm: DNA: 6,600 $M^{-1}cm^{-1}$(per nucleotide), 13,100 $M^{-1}cm^{-1}$(per base pair) [33].

In order to check its purity, the UV absorbance of *Aa*-DNA in the buffer medium was measured at 260 and 280 nm and was found to be free of protein. The DNA binding properties of the test compounds with *Aa*-DNA were investigated by UV–visible spectra. The complex was dissolved in DMSO to obtain the desired concentration. Absorption titration experiments were done by varying the concentration of the *Aa*-DNA, while the complex concentration was kept constant (10 μM). An increasing amount of *Aa*-DNA (10 μL per time) was gradually added to the complex in the buffer after it has been incubated for about 2 h at 25^{o}C. The UV–visible spectra were recorded after equilibration for about 5 min. The intrinsic equilibrium DNA binding constants (K_b) of the complexes to *Aa*-DNA were determined by monitoring the change of the absorption intensity of the spectral bands with increasing concentration of the *Aa*-DNA. The data were then fitted to the following equations to obtain the value of K_b [34, 35].

$$[DNA]/\varepsilon_a - \varepsilon_f = [DNA]/\varepsilon_b - \varepsilon_f + 1/K_b(\varepsilon_b - \varepsilon_f) \quad (1)$$

Where [DNA] is the total concentration of added DNA as M base pairs, ε_a is the apparent absorption in the presence of DNA, ε_f is the extinction coefficient of free Ag(I) complex in the buffer and ε_b is the extinction coefficient of the DNA-bound Ag(I)-NHC complex. The value of ε_f was obtained from a Beer's plot of the Ag(I)-NHC complex while the value of ε_b was obtained from the absorbance of a saturated Ag-DNA sample divided by the concentration ([Ag-NHC]). Plots of [DNA] / (ε_a - ε_f) versus [DNA] were obtained as K_b by the ratio of the slope to the intercept i.e. a plot of [DNA]/(εb – εf) versus [DNA] gave a slope of 1/(εb – εf) and a *y* intercept equal to l/K_b (εb – εf), where K_b is the ratio of the slope to the *y* intercept. Values with a magnitude order of 10^5 M^{-1} for K_b were considered to be indicative of a relatively strong interaction between DNA and metal complexes [36-38]. The non-linear analysis was done using OriginLab version.

2.5.2. DNA binding analysis using viscometric method

Spectroscopic experiments provide many vital information in elucidating the type and strength of the metal complex-DNA interaction with viscometry measurements often considered as the least ambiguous and the most evaluative test of a DNA binding model in solution, clarifying the mode of interaction of a compound with the DNA [39, 40].

DNA viscosity experiments were carried out in Oswald viscometer and the temperature was controlled with a thermostatic water bath set at 29 ± 0.1^{o}C. DNA concentration was kept constant in all samples, while the complex concentration was increased each time, prepared from a stock solution of 2.5 mM. Mixing of the solution was performed by bubbling nitrogen gas through the viscometer in order to aid mixing. A digital stopwatch was used for the measurement of the downward flow of the solution, this was done in triplicate for each sample in order to obtain the mean flow time. Data were presented as $(\eta/\eta_0)^{1/3}$versus the ratio of the compound to DNA concentration, where η is the viscosity of DNA in the presence of

the metal complex and η_0 is the viscosity of the DNA solution, t_f is the experimental flow time per second and t_0 is the flow time of buffer per second [37, 38]. The following equation (2) was employed in the calculation of the ratio $(\eta/\eta_0)^{1/3}$.

$$\eta = \frac{t_f - t_o}{t_o} \quad (2)$$

2.5.3. Nuclease activity assay

The degradation/cleavage ability of the test compounds on DNA was assayed using plasmid (pDs-Red Express) and genomic (*Aa. albopictus* larvae) DNA. The plasmid DNA (pDNA) and genomic DNA (gDNA) were isolated using High Speed Plasmid Mini Kit (Geneaid®) and DNeasy® Blood & Tissue Kit (Qiagen®) according to the manufacturers' instructions.

The constituents of the assay were 1 µL of 50 µg/mL of the test compound (salt/complex), 5 µL of 50 mM Tris-HCl (pH 8.0) and 4 µL of DNA (either pDNA or gDNA). The setup was incubated at 37 ºC for 8 and 24 h. Electrophoresis of 5 µL of the product was conducted on a 0.8 % agarose gel stained with 2.5 µL of Health View Nucleic Acid Stain (Genomics BioSci & Tech) in 0.5X TAE buffer at 70 V for 1 h. The gel was observed under ultra-violet (UV) light and the image was captured in the UVP Gel-Doc-It Imaging System (Kinematics®).

3. **Results and discussion**

3.1. Synthesis

The reaction of *N*-cyanobenzyl or *N*-cyanopropyl benzimidazole with 1-bromopentane and 3-bromomethyl benzonitrile in dioxane under reflux successfully gave the corresponding salts **1a**, **2a** and **3a** in good yield. This was followed by the treatment with KPF_6 salts in methanol to obtain the respective hexafluorophosphate salts (**1b**-**3b**) in good yield. On the other hand bis-benzimidazolium bromide salt **4a** was prepared in good yield by reacting 1,4-bis(bromomethyl)benzene with two equivalents of *N*-cyanobenzylbenzimidazole under reflux in dioxane for 3 days. The pure form of the bromide salt was obtained after recrystallization

from methanol-diethyl ether. The bromide salt **4a** was directly converted to the hexafluorophosphate counterpart (**4b**) with KPF_6 in methanol (Scheme 1). The bromide salts were moisture sensitive and hence, were converted to their more stable hexafluorophosphate counterparts by simple anion exchange reactions. Both mono and bis-benzimidazolium bromide and hexafluorophosphate salts were readily soluble in polar organic solvents such as methanol, ethanol, acetonitrile, DMSO and DMF, but were insoluble in hexane, benzene, toluene and diethyl ether.

The corresponding Ag-NHC complexes (**5b**-**8b)** were prepared *via* the deprotonation of the benzimidazolium salts (Scheme 2) and refluxing the benzimidazolium salts **1b**-**4b** for 1-2 days in the presence of a slight excess of Ag_2O. The mixture was filtered through a pad of Celite® and the filtrate was slowly evaporated to precipitate a white solid. The resulting solid was redissolved in acetonitrile and diethyl ether was added to reprecipitate the solid in good yield and high purity. In general the reaction is summarized in equation 4:

$$2\ \mathrm{NHC.PF_6} \xrightarrow[\mathrm{Ag_2O}]{\mathrm{CH_3CN}} 2(\mathrm{NHC})\mathrm{Ag.PF_6} + \mathrm{H_2O} \qquad 4$$

The Ag(I)–NHC complexes (**5b**-**8b**) were thermally stable up to their melting points and were non-hygroscopic. The complexes were readily soluble in DMSO, DMF and acetonitrile.

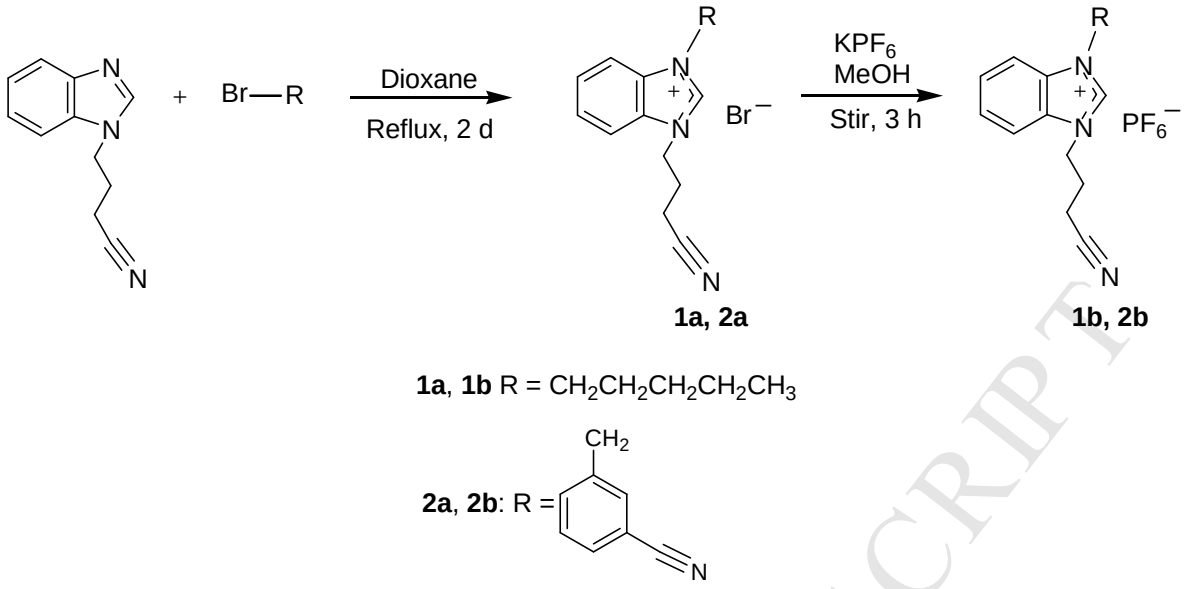

1a, **1b** R = $CH_2CH_2CH_2CH_2CH_3$

2a, **2b**: R =

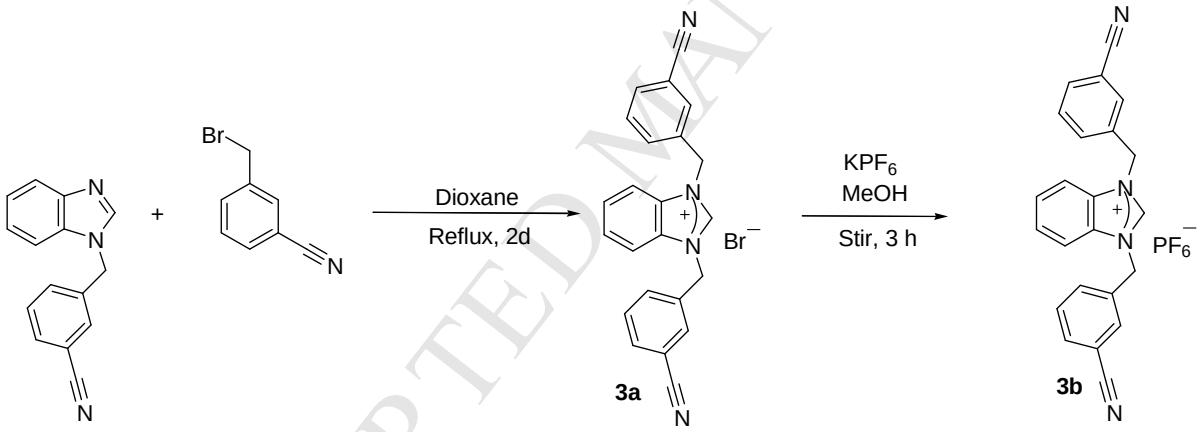

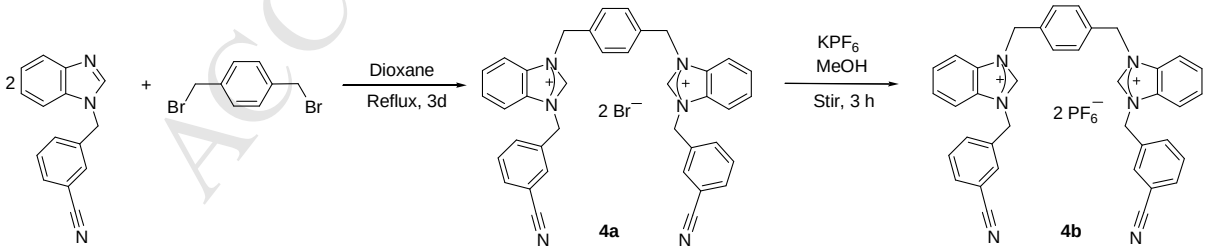

Scheme 1. Synthesis of benzimidazolium halide and hexafluorophosphate salts **1a**–**4a** and **1b**–**4b**

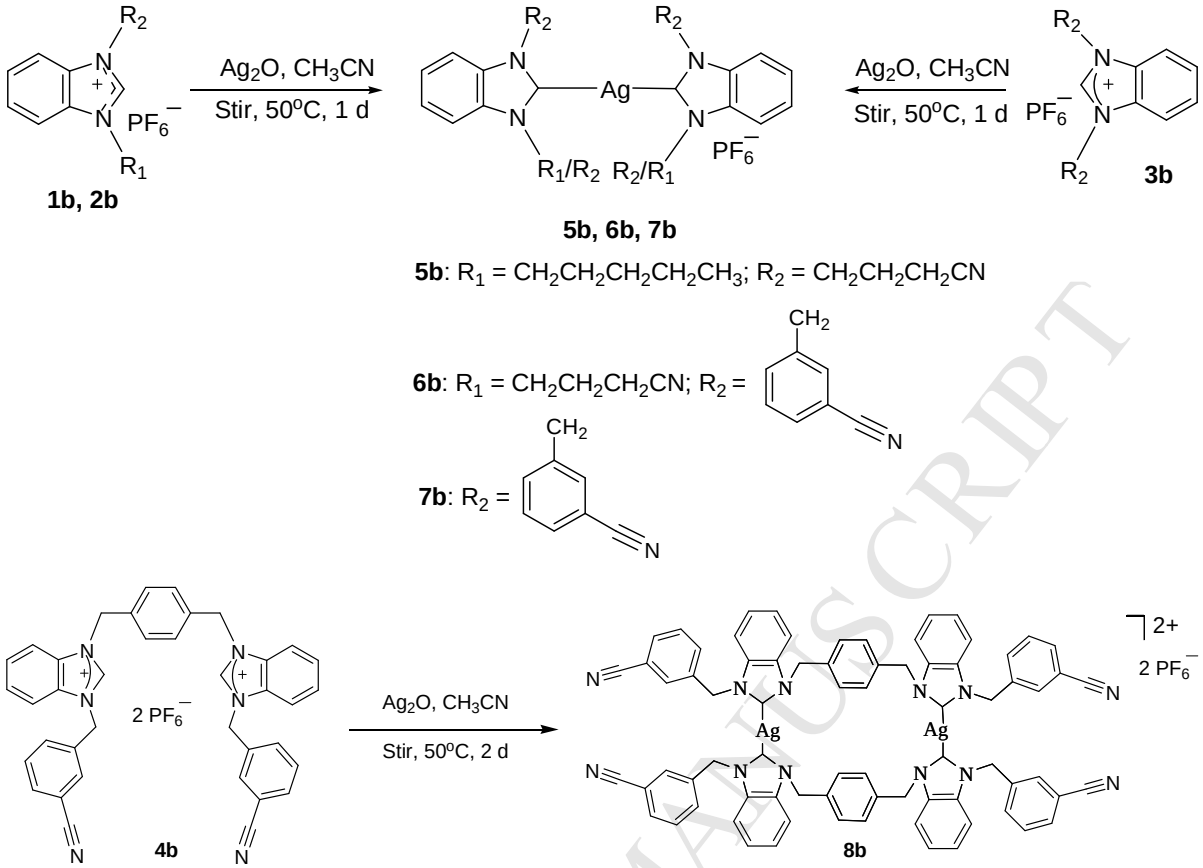

Scheme 2. Synthesis of Ag(I)–NHC complexes **5b**–**8b**.

3.2. Spectroscopy studies

Solution studies was done in order to determine the stabilities of the Ag(I)-NHC complexes. This was performed in D_2O-10% of DMSO-d_6 and 100% DMSO-d_6 and monitored by NMR over a period of seven days. All the investigated Ag(I)-NHC complexes showed no significant changes since their ^{1}H NMR and ^{13}C NMR spectra remained similar. The ^{1}H- and ^{13}C NMR spectra of complexes **5b** and **6b** after 7 days in 10% aqueous DMSO are shown in Figs. S1 and S2, and were identical to the spectra obtained after 15 min (see supplementary data).

In order to further assess the stability of the complexes in the mixture, 10 μg/mL of **5b**-**8b** in DMSO was prepared and added in a 1:1 ratio to the stock solution of the biological medium prepared in DMSO. This was done to imitate the conditions of the *Ae.. albopictus* evaluation

experiments. The complexes used for the testing were dissolved in the minimal amount of DMSO possible and diluted with the medium's stock solution of 10^{-6} M and less than 0.8% DMSO. UV-visible spectra were measured after 0, 24, 48 and 72 h to determine the stability of the complexes. The complexes were stable in the biological medium over the period of the testing time as the UV-visible spectra remained unchanged in 72 h (see supplementary data, Fig. S3).

All the compounds were characterized by elemental analysis, FT-IR, NMR spectrometry, UV-visible spectroscopy, Molar conductivity and X-ray crystallography. FTIR spectra for salts **1b-4b** showed a band of medium intensity in the range 2920–2960 and 3015–3143 cm^{-1}, which is assigned to the pure modes of C-H stretching vibrations. This is due to the presence of aliphatic and aromatic C-H modules respectively and they were present in all the Ag-NHC complexes (**5b**-**8b**) with some negligible changes [41]. A sharp band at 2229–2249 cm^{-1} is assigned to *ν* (C≡N) of the nitrile functionality [41] and remained unaltered in the complex spectra. This is an indication of their presence outside the coordination sphere as a result of the coordinative saturated metal centers. A sharp and medium intensity band appeared in the range 1432–1568 cm^{-1}, which is due to the benzimidazole ring C=N stretching vibrations. Interestingly, in the spectra of the Ag-NHC complexes, bands corresponding to the stretching vibrations of the benzimidazole ring C=N modules shifted towards the lower energy side compared with their salts (Figs. S4-S7, supplementary data). Further evidence for the formation and structures of these complexes were provided by elemental analysis, NMR spectroscopy, Molar conductance and X-ray crystallography.

In the ^{1}H NMR spectra of **1a**-**4a**, resonances for the benzimidazole, the benzonitrile, and the alkyl protons were observed. The presence of a singlet at 9.99, 10.15, 10.21 and 10.15 ppm corresponding to the NC*H*N benzimidazolium protons confirmed the formation of **1a**, **2a**, **3a** and **4a** respectively. This is quite consistent with those of other benzimidazole based NHC

precursors [41, 42]. In addition, the resonances of aliphatic protons of alkyl chain were consistent in the ranged ca. 0.89–5.95 ppm, which is in agreement with similar structures found in the literature [41]. The salts also showed similar spectra in the aromatic area in the range of 7.48 - 8.20 ppm. Furthermore, the ^{13}C NMR spectroscopy displayed Benzimidazolium-C2 carbon resonances in the range ca. 137.5-143.5 ppm. Metathesis reactions of these salts with KPF_6 in methanol afforded **1b**-**4b** in good yield. In the ^{1}H NMR spectra, no changes were observed in relation to **1a** -**4a**.

Upon Ag-NHC complex formation, the ^{1}H NMR spectra of complexes **5b**−**8b** supported the formation of the envisioned NHC complexes by the absence of any signals around δ = 10 ppm attributable to the acidic protons at the C2 position of the benzimidazolium moieties. Apart from this, the spectra of all the complexes were more or less similar to their corresponding salts. On the other hand, ^{13}C NMR spectra of complexes **5b**, **7b** and **8b** evidenced the presence of a non-ligand signal in the most downfield region at ca. 188.3–190.8 ppm ascribed to the carbene carbon resonances due to the formation of Ag-C bond. In contrast, **6b** displayed resonances for the C2-carbon nuclei as two doublets centred at δ (189.2 and 190.4) as a result of ^{13}C-^{107}Ag and ^{13}C-^{109}Ag coupling constants of 185 and 205 Hz, respectively. Also, signals in the range δ 7.32-8.01 ppm in all spectra were assigned to the aromatic protons.

The intensive absorption peaks at 277-281 and 285-287 nm can be assigned to π-π* and *n*-π* orbital transition of the salts and the complexes respectively, originating from the C═C and C═N modules [43]. These transitions were also observed in the spectra of the complexes but were shifted to a higher wavelength as a result of complexation with Ag(I). However, no bands at the lower energy level for d–d transition were detected in the UV–visible region. An overlay of the electronic spectra for the salts and the corresponding complexes are shown in fig1.

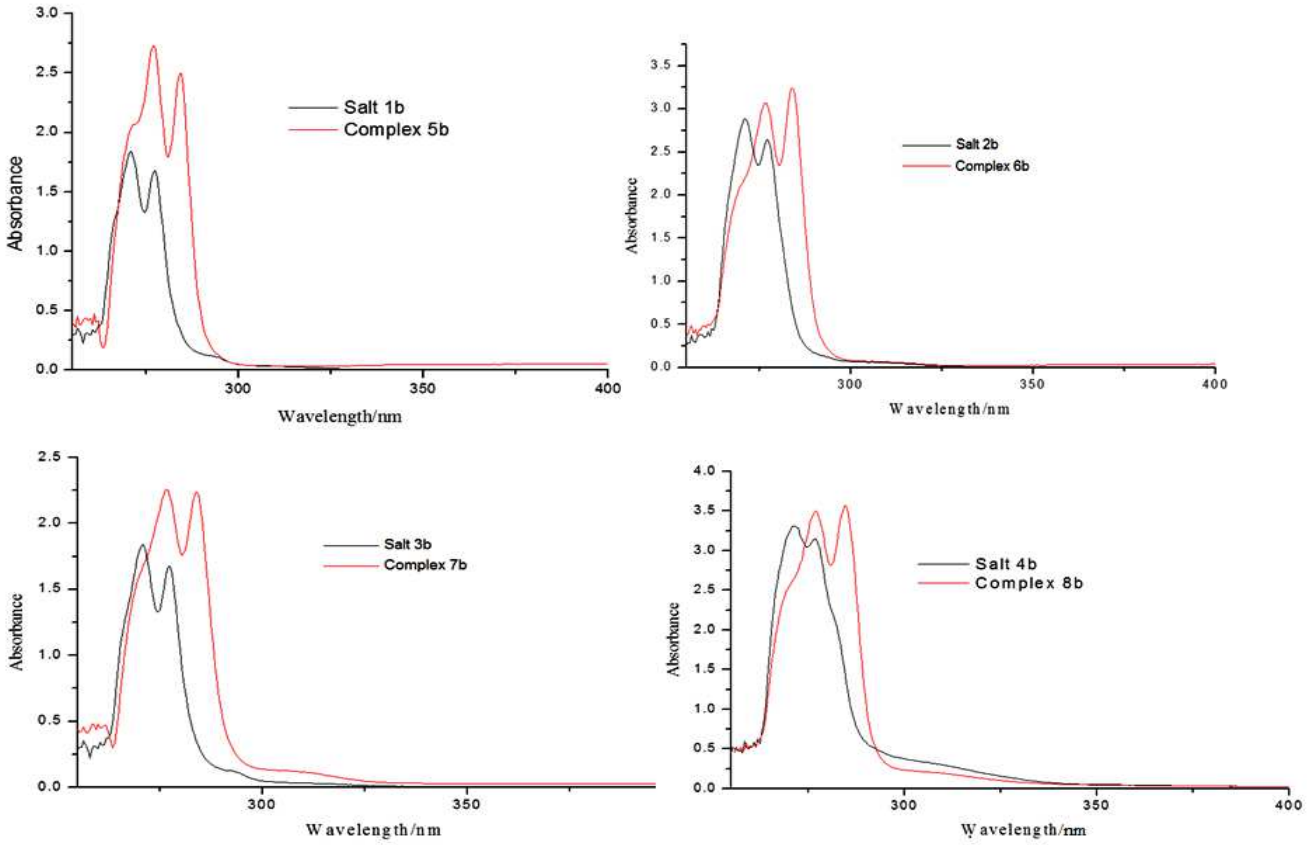

Fig 1. Overlays of absorption spectra of the four salts (**1b**-**4b**) and their corresponding Ag–NHC complexes (**5b**–**8b**) studied in this work

3.3. Molar conductivity measurements

The molar conductance values of the benzimidazolium salts and complexes were obtained at room temperature in DMF solution at 10^{-3} M concentration. The compounds were dissolved in DMF and the molar conductivities of their solutions at 25 ± 2 °C were measured. The molar conductivity values of the benzimidazolium salts **1b**-**3b** and their Ag(I)–NHC complexes **5b**-**7b** were found to be close, at around 24.76–27.78 S cm^2 mol^{-1}, indicating the ionic nature of these compounds, which were found to be 1:1 electrolytes [44]. On the other hand, salt **4b** and its Ag(I)–NHC complex **8b** values were almost double (**4b** at 52.67 and **8b** at 59.25 S cm^2 mol^{-1}), indicating that they were 2:2 electrolytes. Based on the foregoing, we could also deduce the structure of the compounds on the basis of their molar conductance. It is obvious from this study that each mononuclear Ag(I)–NHC complex has one

hexafluorophosphate counterion to balance the Ag^+ and as a consequence reflects the formation of a mononuclear Ag–NHC complex. However **4b** and **8b** have two hexafluorophosphate counterions to balance the two Ag^+ and as a consequence indicates the formation of a tetracarbene complex. The molar conductivity data, elemental analysis and spectroscopy data show an agreement with the proposed structure of the compounds, which was further confirmed by means of the data obtained by single crystal X-ray diffraction.

3.4. Single crystal X-ray diffraction studies

Complex **8b** crystallized in triclinic *P*-1 space group with half of the molecule in the asymmetric unit (Figure 2). The presence of two hexafluorophosphate anions in the lattice then balances the entire charge. Both Ag(I) were in linear geometry, with the angle of C15-Ag1-C30i being 176.84(16)^o. The distances of Ag1-C15 and Ag1-C30^i were 2.092(5) Å and 2.091(5) Å, respectively (Table 2). The packing diagram of the molecule is dominated by the presence of π-π interaction between the aromatic rings.

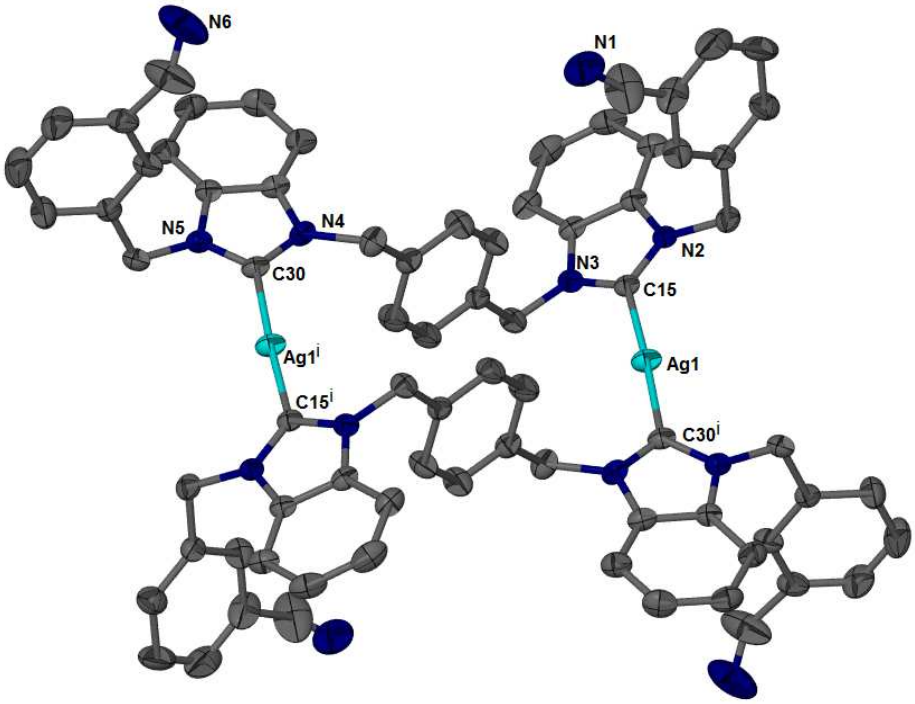

Fig 2: Structure of **8b** with ellipsoids shown at 50% probability. Hydrogen atoms and PF_6^- anions in the lattice omitted for clarity. Symmetry element used: ^{i} = 1-x, 2-y, 1-z.

Table 1

Selected bonds lengths (Å) and angles (^{O}) of **8b**

Ag1-C15	2.092(5)
Ag1-C30^{i}	2.091(5)
C15-Ag1-C30	176.84(6)
N2-C15-N3	105.8(4)
N4-C30-N5	105.7(4)

3.5. Antibacterial Activities

The antibacterial activities of the complexes were described by the disc diffusion, MIC, MBC and colony formation methods. The antibacterial activity showed good to moderate activity. The results obtained by the Kirby-Bauer's disc diffusion method were comparable with that of the MIC values (Tables 2a, 2b and 3). In a solvent control test, the role of DMSO was studied and it was observed that 10 % DMSO did not have any inhibitory activity on the growth of microorganisms [45]. The antibacterial activities of compounds **1b**-**8b** were screened against 2 isolated pathogens (*E. coli* and *S. aureus*). The MICs of the compounds were compared to the MICs of $AgNO_3$ and Ciprofloxacin.

All complexes in this study were effective at inhibiting the growth of *E. coli* and *S. aureus* while their corresponding salts were inactive against both strains of bacteria [46]. The MIC values of the complexes against both *E. coli* and *S. aureus* were in the range of 25-100 μg/mL. These Ag(I)-NHC complexes (**5b-8b**) had better antibacterial qualities in comparison with silver nitrate. The bis–NHC–Ag(I) complex (**8b**) exhibited promising antibacterial activity. This complex (**8b**) displayed impressive antibacterial potential against *S. aureus* at a concentration of 12.5 μg/mL. The complexes showed bacteriostatic effect against both bacteria strains in the range of 12.5 - 100 μg/mL but the bactericidal activity was only in the range of 50 - 200 μg/mL (Table 4; Figs. S9 and S10).

In general, most of the complexes displayed lower inhibitory activities than ciprofloxacin, and the susceptibility levels of the gram-negative and gram-positive bacteria to the complexes were the same except complex **8b** which showed a higher activity against the gram-positive bacteria. Furthermore, the sensitivity of the bacteria strains increases as the concentration of the complex suspensions increases (Table 2a and 2b).

The colony formation studies were evaluated using different concentrations of the tested Ag(I)-NHC complexes. For *E. coli*, the colony forming unit per mL (CFU/mL) decreases as the concentration of the complexes increases. Complex **8b** showed no viable colony of both *E. coli* and *S. aureus* at a concentration of 100 µg/mL (Table 4), which is only comparable to that of the ciprofloxacin. All the other complexes showed different values at concentrations of 100 and 200 µg/mL and no viable colony was observed at concentrations of 200 and 400 µg/mL except for **7b** which had activity at 400 µg/mL only (Table 4).

Table 2a
Antibacterial activities of the compounds[a] against *E. coli* obtained by the disc diffusion method (zone of inhibition ± SD/mm)

Test Compound	Inhibition Zone (mm)			
	25 µg/mL	50 µg/mL	100 µg/mL	200 µg/mL
5b	12.5±0.0	12.8±0.5	15.1±0.5	19.0±1.0
6b	11.0±0.7	11.8±1.0	13.2±0.0	15.8±1.5
7b	10.2±0.3	10.8±0.0	12.0±0.0	14.8±0.0
8b	22.6±1.0	24.0±1.0	27±1.5	28.6±0.5
$AgNO_3$	10.8±0.0	11.8±0.0	14.8±0.0	16.8±0.0
Ciprofloxacin	26.3±0.0	26.3±0.0	28.7±0.0	31.0±0.0

[a] : Compounds **1b**- **4b** showed no activity.

Table 2b

Antibacterial activities of the compounds[a] against *S. aureus* obtained by the disc diffusion method[b] (zone of inhibition ± SD/mm)

Test Compound	Inhibition Zone (mm)			
	25 µg/mL	50 µg/mL	100 µg/mL	200 µg/mL
5b	13.5±0.0	13.5±1.0	15.6±0.0	20.9±1.5
6b	11.0±0.0	11.8±1.5	14.2±0.5	17.8±1.0
7b	10.6±0.8	10.8±0.4	12.5±0.0	14.0±1.0
8b	22.6±1.0	23.0±1.0	27.8±0.5	29.6±0.5
$AgNO_3$	10.8±0.0	11.8±0.0	14.8±0.0	16.8±0.0
Ciprofloxacin	26.3±0.0	26.3±0.0	29.7±0.0	32.0±1.0

[a] : Compounds **1b- 4b** showed no activity.

Table 3

Minimum inhibitory concentration (MIC) of the compounds against *E.coli* and *S.aureus*.

Test Compound	*E. coli* (µg/mL)		*S. aureus* (µg/mL)	
	MIC	MBC	MIC	MBC
5b	50	100	50	100
6b	100	200	100	200
7b	100	200	100	200
8b	25	50	12.5	50
$AgNO_3$	100	200	100	200
Ciprofloxacin	6.25	9.38	6.25	12.5

Compounds **1b- 4b** showed no activity.

Table 4
Colony forming unit per ml (CFU/mL) of different concentrations of the complexes against *E. coli/S. aureus*

CFU/mL (10^5)				
Test Compound	Concentration (μg/mL)			
	50	100	200	400
5b	17 ± 1.8/16 ± 1.0	7 ± 1.0/6.5 ± 1.5	0	0
6b	19 ± 0.7/17 ± 0.0	8 ± 0.5/7 ± 1.0	0	0
7b	20 ± 1.0/18 ± 1.5	11 ± 1.8/9.5 ± 1.0	3 ± 1.8/16 ± 1.0	0
8b	7 ± 1.5/5 ± 0.5	0	0	0
$AgNO_3$	18 ± 0.5/17 ± 2.0	8 ± 0.8/6.8 ± 0.0	0	0
Ciprofloxacin	3 ± 0.0/3 ± 0.0	0	0	0

3.6. DNA binding

UV-Vis absorption spectroscopy can be used to observe possible intercalation interactions between *Aa*-DNA and the Ag(I)–NHC complexes. In addition, viscosity measurements were also performed in order to further evaluate the nature of DNA interaction with the complexes. An intercalative mode involves a strong stacking interaction between the aromatic chromophore and the base pair of DNA, thus a complex binding to DNA through intercalation usually results in hypochromism and bathochromism [47, 48]. Compounds **5b**–**8b** were allowed to interact with *Aa*-DNA and the interactions were investigated by UV–visible spectra in phosphate buffer (10 mM, pH = 7.4) containing 50 mM NaCl at 25 °C. As illustrated in Fig. 3 and Table 5, with increasing concentration of *Aa*-DNA, the absorption intensities of these compounds were reduced by a large hypochromicity of 28 and 32% and smaller hypochromicity of 18 and 21%. Bathochromic shift was not observed in the spectra and the maximum absorption showed obvious hypsochromic adsorption (7.0–11.5 nm). As a

result of the reduced absorbance and the hypsochromic shift, an intercalative binding mode is assigned to these complexes. The values of K_b and site sizes were obtained from the spectroscopy emission data and these data were fitted to the equation previously derived [49] and were calculated to be 2.177×10^6, 8.672×10^5, 6.665×10^5 and 3.627×10^6 (**5a**, **6b**, **7b**, **8b**) respectively. The absorbance titration showed the binding site size (s) between 0.71 and 1.16, which correspond to a binding stoichiometry of about one Ag–NHC complex per base pair site. The K_b values showed that compound **8b** with a bimetallic center has the highest binding constant and consequently manifests the strongest binding properties with *Aa*-DNA compared to the mononuclear counterparts. In general the mode of action is linked to a strong stacking interaction between the planar aromatic chromophore and the intercalating agents [50].

Values of K_b obtained from the absorption titrations in the present work are in reasonable agreement with those obtained from DNA titrations of similar complexes in the literature [51–54]. In addition, the results of the interactions of benzimidazolium salts with DNA in literature showed that the K_b values are quite less than those of the corresponding Ag complexes [51–55].

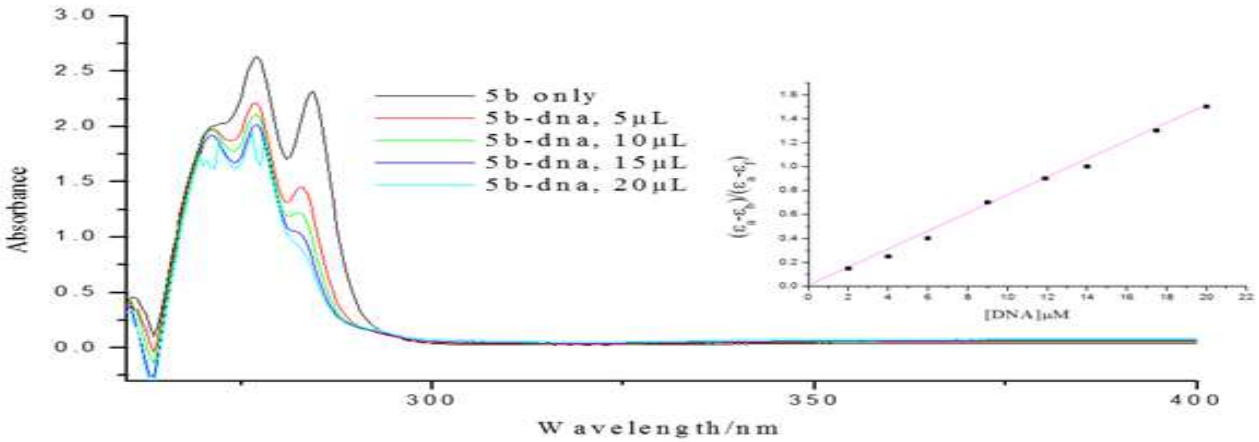

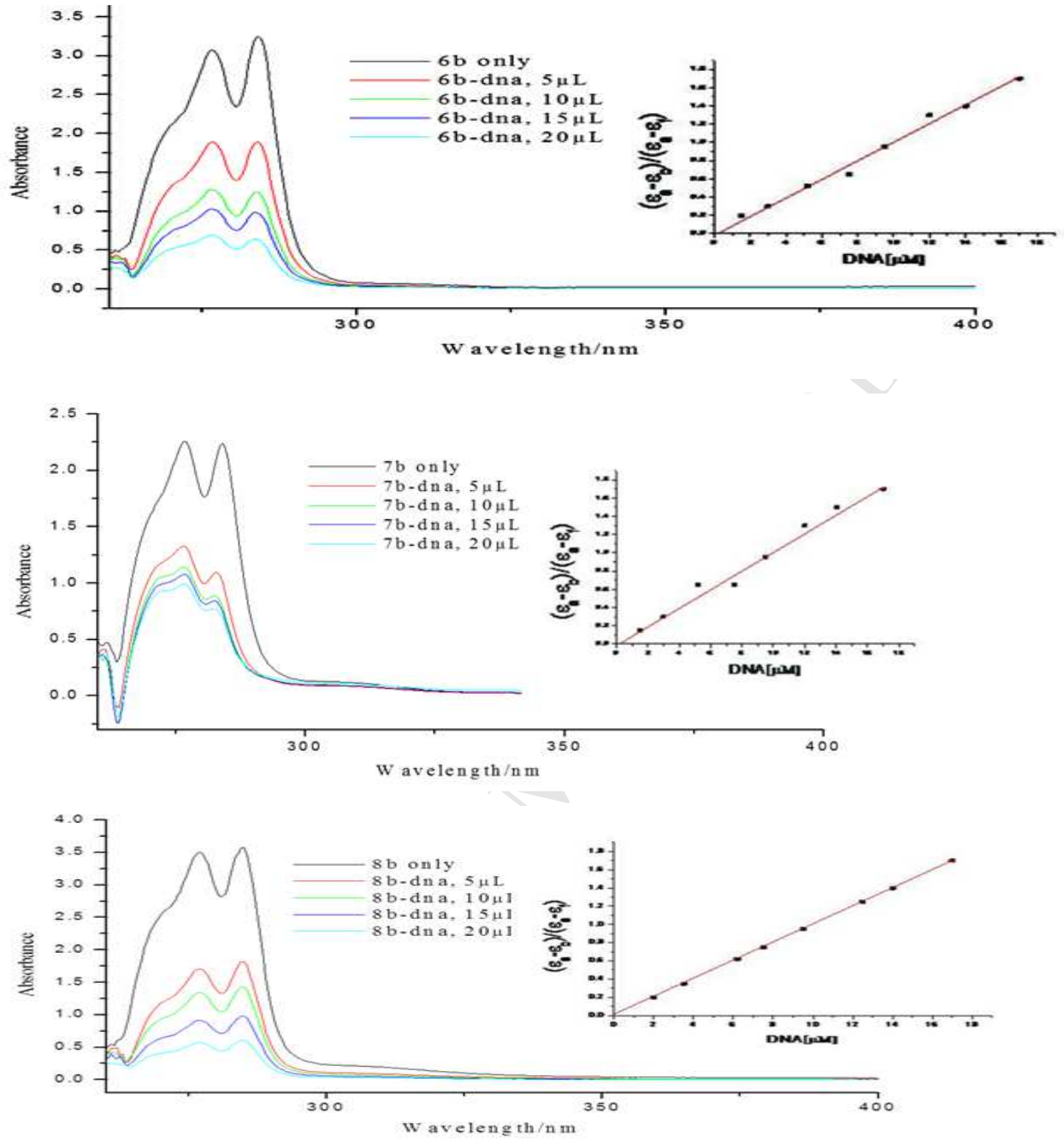

Fig. 3. Absorption titrations of complexes **5b-8b** with increasing amounts of *Aa*- DNA under conditions listed in Table 5. For each Ag-NHC complex, the spectral series show a progression of decreasing intensity with increasing [DNA]/[Ag]. The inset shows the plot of Δεa/Δεb vs [DNA],
obtained from absorption spectral titration of the complexes.

Table 5
DNA Binding Constants for Ag-NHC Complexes **5b**-**8b**[a]

Complex	Hypsochromic Shift (nm)	K_b[b]	S[b]	%H[c]
5b	11.5(277)	2.177×10^6	0.90	28%
6b	7.0(273)	8.672×10^5	0.71	21%
7b	11.0(284)	$6.665. \times 10^5$	0.64	18%
8b	10.0(285)	3.627×10^6	1.16	32%

[a] Conditions: 10 mM phosphate pH 7.4, 50 mM NaCl, **5b**-**8b**.
[b] Error in K_b and s values from Absorption titrations are $\pm 0.6 \times 10^6$ and ± 0.05. Where k_b = DNA binding constants and s = binding site sizes.
[c] Percent hypochromicity at specified wavelength in the absorption spectrum, The percentage hypochromicity was calculated using equation (4) [55].

$$\% H = (A_a - A_b/A_a) \times 100 \quad (4)$$

Where A_a is the absorbance (free metal complex) and A_b is the absorbance at 260 nm (mixture of metal complex bound to DNA).

3.7. DNA Binding Activity Using Viscometry

The change in length as a result of an interaction between DNA's double helix and a small molecule is an unambiguous method to study DNA viscosity. An intercalative metal complex induces a detachment of the base pairs, so that it can be fitted to the DNA structure, therefore generating the lengthening of the nucleic acid helix and an increase in its viscosity [40]. On the other hand the metal complex can bend or kink the DNA double helix due to a partial and/or non-classical intercalation. This reduces its effective length and consequently reduces the DNA viscosity [56].

The result of the viscosity titration plots is shown in Fig. 4. The viscosity of *Aa*-DNA increased with an increase in the concentration of the added complexes. This indicates the lengthening of the DNA duplex following the intercalative DNA binding of the complex. Positive slopes were observed for all the complexes, although with values less than that for proven intercalating agent [57]. As a result of the foregoing, the result also showed an appreciable intercalating mode of the interactions of these complexes [58].

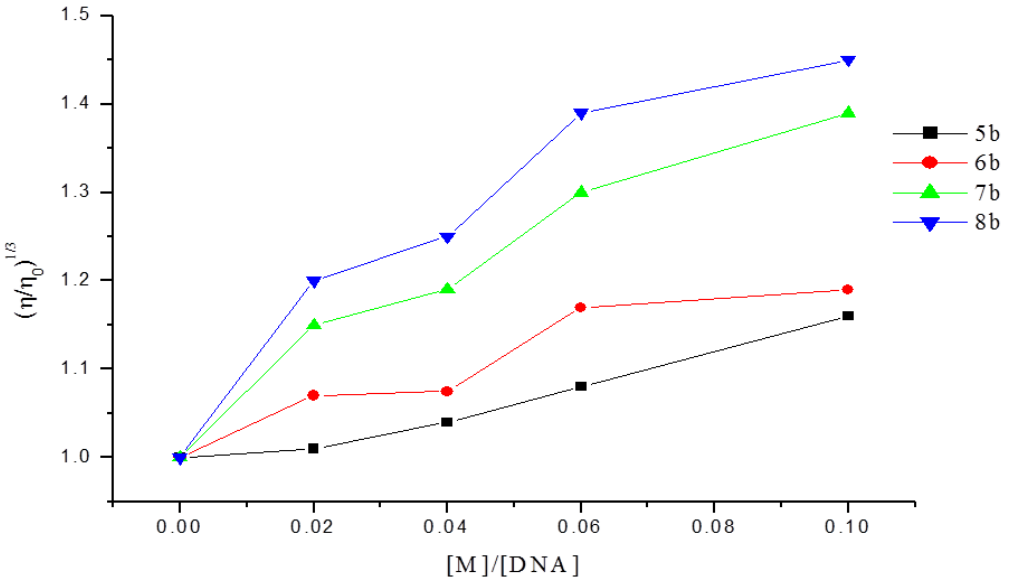

Fig 4. Viscosity titration of *Aedes albopictus*-DNA and each of the four Ag-NHC complexes at10 mM phosphate buffer pH 7, 50 mM NaCl, [Ag] 25 µM.

3.8. Deoxyribonuclease (DNase) activity of test compounds

DNA nuclease activity of the compounds was assessed using pDNA and *Ae. albopictus* gDNA. An 8 h incubation of the compounds with pDNA did not exhibit any noticeable nuclease activity of either the complexes or salts (Fig. 5). After a prolonged incubation of 24 h, no cleavage or degradation activity of pDNA by the salts was observed (Fig. 6). However, a little degradation (smear) was observed in the reaction using the complexes (Fig. 6).

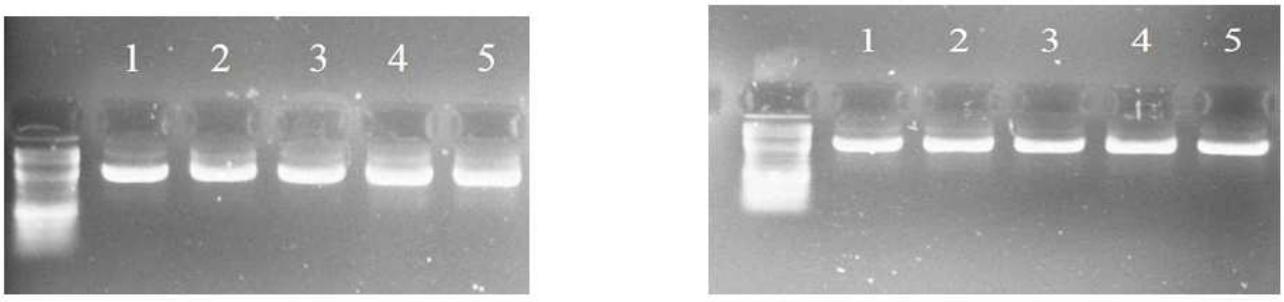

A B

Fig 5. Agarose gel analysis of pDNA after 8 h incubation at 37 °C with the test compounds. (A) pDNA incubated with Complexes. Lane 1: pDNA only; Lane 2: pDNA + **5b**; Lane 3:

pDNA + **6b**; Lane 4: pDNA + **7b**; Lane 5: pDNA + **8b**. (B) pDNA incubated with Salts. Lane 1: pDNA only; Lane 2: pDNA + **1b**; Lane 3: pDNA + **2b**; Lane 4: pDNA + **3b**; Lane 5: pDNA + **4b**.

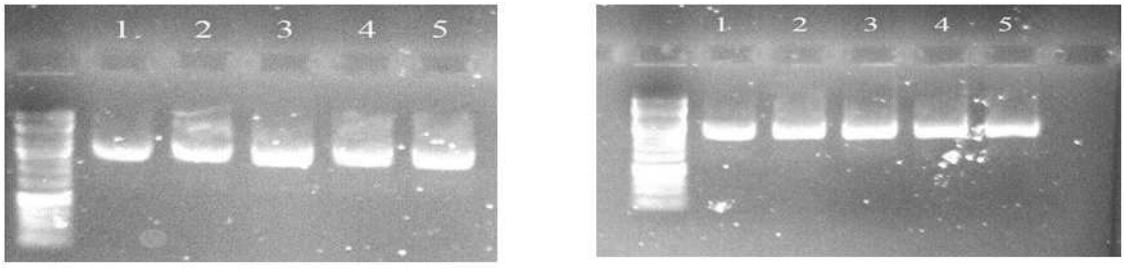

A B

Fig 6. Agarose gel analysis of pDNA after 24 h incubation at 37 °C with the test compounds. (A) pDNA incubated with Complexes. Lane 1: pDNA only; Lane 2: pDNA + **5b**; Lane 3: pDNA + **6b**; Lane 4: pDNA + **7b**; Lane 5: pDNA + **8b**. (B) pDNA incubated with Salts. Lane 1: pDNA only; Lane 2: pDNA + **1b**; Lane 3: pDNA + **2b**; Lane 4: pDNA + **3b**; Lane 5: pDNA + **4b**.

The compounds (complexes/salts) did not exhibit any degradation effect on *Ae. albopictus* gDNA after an 8 h incubation period (Fig. 7). Nuclease activity of the compounds after an incubation time of 24 h showed some degradation effect on the mosquito's gDNA (Fig. 8). Results of the nuclease activity indicate an incubation time-dependent activity in complex-pDNA and complex-gDNA reactions. This is consistent with the time-dependent nucleasing activity of DNA by metal complexes reported by Asekunowo et al. [38]. Since the complexes have better binding abilities for *Ae. albopictus* gDNA, it is likely they bind to the gDNA and induce it to degrade. Degradation of the nucleic acid by these complexes may contribute towards the observed mortality induced in the mosquito. It is also possible that by binding to the gDNA, the complexes interfere with normal functions of the DNA to disrupt biological processes of the mosquito which can have detrimental consequences on the development and survival of the mosquito.

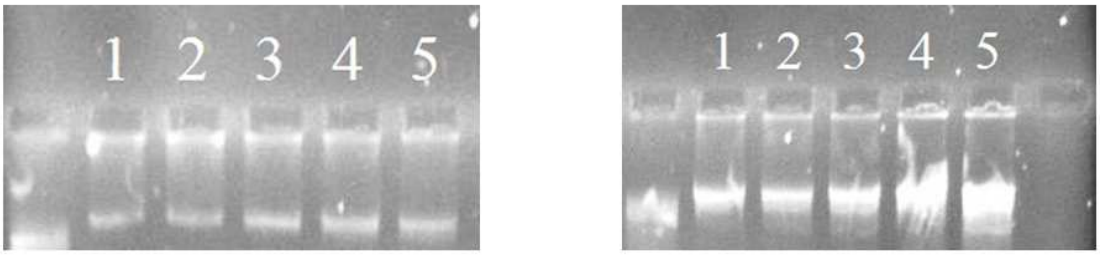

A B

Fig 7. Agarose gel analysis of *Aedes albopictus* gDNA after 8 h incubation at 37 °C with the test compounds. (A) gDNA incubated with Complexes. Lane 1: gDNA only; Lane 2: gDNA + **5b**; Lane 3: gDNA + **6b**; Lane 4: gDNA + **7b**; Lane 5: gDNA + **8b**. (B) gDNA incubated with Salts. Lane 1: gDNA only; Lane 2: gDNA + **1b**; Lane 3: gDNA + **2b**; Lane 4: gDNA + **3b**; Lane 5: gDNA + **4b**.

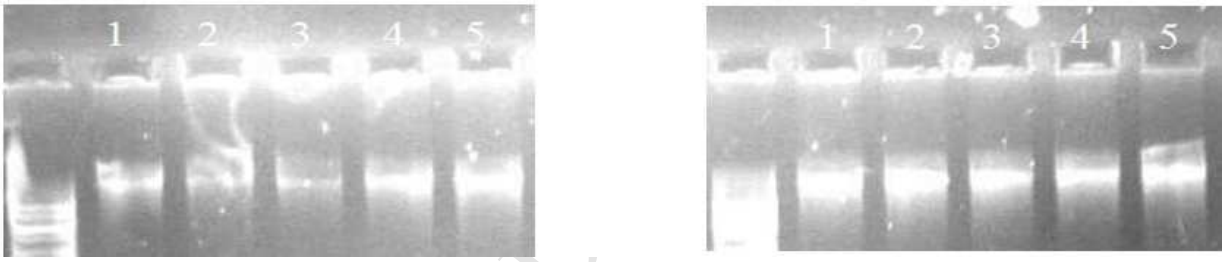

A B

Fig 8. Agarose gel analysis of *Aedes albopictus* gDNA after 24 h incubation at 37 °C with the test compounds. (A) gDNA incubated with Complexes. Lane 1: gDNA only; Lane 2: gDNA + **5b**; Lane 3: gDNA + **6b**; Lane 4: gDNA + **7b**; Lane 5: gDNA + **8b**. (B) gDNA incubated with Salts. Lane 1: gDNA only; Lane 2: gDNA + **1b**; Lane 3: gDNA + **2b**; Lane 4: gDNA + **3b**; Lane 5: gDNA + **4b**.

3.9. Larvicidal effect of test compounds on Aedes albopictus larvae

Many conventional insecticides and other insecticide-based products for mosquito control are failing to achieve the desired level of efficacy due to the development of insecticide resistance [59, 60]. The resistance to conventional insecticides and factors like the global spread of *Ae. albopictus* and the prevalence of *Aedes*-transmitted diseases underpin the need for effective mosquitocidal compounds to impede the spread of *Ae. albopictus*-borne

diseases. Toxicity of the test compounds against fourth instar larvae of *Ae. albopictus* (Fig. S11) shows that LC_{50} of the salts were significantly different ($p<0.05$) from the complexes (Fig. S12, Table 6). However, the LC_{50} values were not significantly different among the salts (Fig. S11, Table 6). In contrast, LC_{50} values of the complexes were significantly different from each other ($p<0.05$), except complexes **6b** and **7b** (Fig. S12, Table 6). The LC_{50} of the complexes were about 40 to 95-fold lower than that of the salts (Table 6). Based on the classification of Cheng et al. [61], complexes **5b**, **6b** and **8b** were considered highly active against the larvae while complex **7b** was considered active (Table 6). However, all the salts were inactive against the larvae.

Similar to their LC_{50} values, the LC_{90} values of the salts were not significantly different ($p>0.05$) from each other but were significantly different ($p<0.05$) from that of the complexes (Figs. S11 and S12, Table 6). The toxicity results show that *Ae. albopictus* larvae treated with the synthesized compounds were more tolerant to the salts compared to the complexes. LC_{50} and LC_{90} of complex **8b** was the lowest among the complexes and approximately 3 to 5-fold and 4 to 6-fold lower respectively than that of the other complexes (Table 6). This shows that complex **8b** was more toxic to the fourth instar larvae of the mosquito compared to the other test compounds. The positive reference, temephos (1 ppm), induced 100% larval mortality in this study. However, resistance to temephos has developed in some *Aedes* populations [59, 62, 63] and this adversely affects temephos-based vector control. Although the complexes were less toxic than the positive reference, they displayed high larvicidal activity against the mosquito, especially complex **8b**. The observed toxicity of the complexes in this test was high compared to organotin(IV) and tetra-coordinated tin(II) complexes evaluated on larvae of *Ae. aegypti* [64]. The complexes also exhibited high larvicidal activity compared to thiadiazolo derivatives (LC_{50} of 21.7 to 102.8 ppm) assayed on *Anopheles stephensi* [65] and thiosemicarbazones derivatives (LC_{50} of 5.8 to >200 ppm) assayed on *Ae. aegypti* [66]. The

emergence of temephos resistance in *Aedes* mosquitoes [59, 62] and the demand for newer, effective and environmentally friendly anti-mosquito compounds make these complexes worthy candidates as potential larvicidals.

However, the toxic effects of the complexes on *Ae. albopictus* larvae were lesser compared to triganothin dithiocarbamates on *Ae. aegypti* and *An. stephensi* [67]. Although most of the compounds in that study [67] outperformed the complexes in this study, complex **8b** performed better compared to NH(n-Bu) (LC_{50}=13.74) and NH(n-Pr) (LC_{50}=11.94). Mosquito species respond differently to chemical compounds [67], so the relatively low LC values of complex **8b** on the *Ae. albopictus* mosquito shows its potential as a larvicide compared to the other complexes.

Table 6

Toxicity of compounds on fourth instar larvae of *Aedes albopictus*

Compound	LC_{50} (ppm)	95% CI	LC_{90} (ppm)	95% CI	Slope ± SE	Larvicidity*
5b	33.32[a]	28.89-38.43	113.44[a]	92.33-139.37	1.79 ± 0.15	Highly active
6b	45.35[c]	40.51-50.77	115.61[ac]	96.81-138.06	2.35 ± 0.20	Highly active
7b	56.44[c]	50.07-63.62	165.17[c]	135.76-200.80	2.05 ± 0.17	Active
8b	11.68[b]	9.92-13.75	27.73[b]	22.82-33.70	2.54 ± 0.22	Highly active
1b	2485.34[d]	438.87-14075.63	9974.15[d]	620.24-160411.87	1.58 ± 0.62	Inactive
2b	1820.59[d]	368.96-8983.10	5406.39[d]	428.38-68234.12	2.02 ± 0.91	Inactive
3b	3036.60[d]	345.09-26720.87	12271.97[d]	413.27-364397.29	1.57 ± 0.71	Inactive
4b	1110.41[d]	370.63-3326.91	2396.79[d]	397.66-14446.39	2.86 ± 1.35	Inactive

Values with different alphabets in the same column are significantly different based on non-overlapping 95% CI.

LC: Lethal Concentration; CI: Confidence Intervals; SE: Standard Error

*Based on the classification of Cheng et al [61] which considers LC_{50}<50 ppm as highly active, LC_{50}<100 ppm as active and LC_{50}>100 ppm as inactive.

3.9.1. Developmental consequences of test compounds on Aedes albopictus

Effect of the compounds on developmental progression of larvae to the adult stage was observed after treatment with three different concentrations of the test compounds. Developmental outcomes such as larval survival and mortality, pupal survival and emerged adults of the treated larvae were significantly different ($p<0.05$) (Tables 7-9).

Treatment with the highest test concentration of 25 ppm induced various developmental consequences on the mosquito, affecting the developmental progression of larvae to the adult stage. Complex **8b** (25 ppm) was lethal to the treated larvae, inducing total mortality and thus terminating developmental progression to the pupal stage (Table 7). This effect is a reflection of the observed toxicity (LC_{50} and LC_{90}) of complex **8b** in the larvicidal study and corroborates the high larvicidal potential of this complex. About 8% of larvae treated with 25 ppm of complex **7b** successfully emerged as adults. Although 20% larval mortality was observed in complex **7b**-treated larvae, about 72% survived but were still in the larval stage. The proportion of emerged adults from larvae treated with the salts were higher (16-28%) than those treated with the complexes (0-12%; Table 7).

Table 7
Developmental consequences of test compounds (25 ppm) on *Aedes albopictus* larvae

Compound	Larvae		Pupae		Emerged
	Alive ± SE (%)	Dead ± SE (%)	Alive ± SE (%)	Dead ± SE (%)	Adults ± SE (%)
5b	52.0±4.6^{ab}	4.0±2.3^{a}	32.0±8.3^{a}	0.0±0.0	12.0±2.3^{abc}
6b	40.0±10.1^{ad}	0.0±0.0^{a}	48.0±10.6^{ac}	0.0±0.0	12.0±6.1^{abc}
7b	72.0±14.0^{b}	20.0±10.1^{c}	0.0±0.0^{b}	0.0±0.0	8.0±4.0^{bc}
8b	0.0±0.0^{c}	100.0±0.0^{b}	0.0±0.0^{b}	0.0±0.0	0.0±0.0^{b}
1b	36.0±16.2^{ad}	0.0±0.0^{a}	48.0±14.4^{ac}	0.0±0.0	16.0±6.1^{abc}
2b	36.0±13.9^{ad}	0.0±0.0^{a}	44.0±6.1^{ac}	0.0±0.0	20.0±8.3^{ac}
3b	20.0±9.2^{cd}	0.0±0.0^{a}	64.0±14.4^{c}	0.0±0.0	16.0±6.1^{abc}
4b	24.0±11.5^{acd}	0.0±0.0^{a}	48.0±6.1^{ac}	0.0±0.0	28.0±6.1^{a}
DMSO	20.0±2.3^{cd}	0.0±0.0^{a}	52.0±6.1^{ac}	0.0±0.0	28.0±8.3^{a}

Values with different alphabets in the same column are significantly different at $p<0.05$.
SE: Standard Error

In larvae treated with 5 ppm of the test compounds (Table 8), about 4-32% emerged as adults (4-24% for complexes and 24-32% for salts). Larval mortality was only observed in complexes **5b** and **8b**-treated larvae. The highest proportion of survived larvae was observed in those treated with complexes **7b** and **8b** (Table 8).

Table 8

Developmental consequences of test compounds (5 ppm) on *Aedes albopictus* larvae

Compound	Larvae		Pupae		Emerged
	Alive ± SE (%)	Dead ± SE (%)	Alive ± SE (%)	Dead ± SE (%)	Adults ± SE (%)
5b	44.0 ± 6.1^{a}	4.0 ± 2.3^{a}	32.0 ± 4.0^{ab}	0.0 ± 0.0	20.0 ± 8.3^{abcd}
6b	24.0 ± 4.0^{b}	0.0 ± 0.0^{c}	52.0 ± 14.0^{abc}	0.0 ± 0.0	24.0 ± 10.1^{abcd}
7b	56.0 ± 10.6^{a}	0.0 ± 0.0^{c}	32.0 ± 10.6^{ab}	0.0 ± 0.0	12.0 ± 4.0^{bc}
8b	56.0 ± 8.3^{a}	16.0 ± 2.3^{b}	24.0 ± 10.6^{a}	0.0 ± 0.0	4.0 ± 4.0^{b}
1b	8.0 ± 4.0^{bc}	0.0 ± 0.0^{c}	68.0 ± 10.6^{c}	0.0 ± 0.0	24.0 ± 10.6^{abcd}
2b	16.0 ± 2.3^{bc}	0.0 ± 0.0^{c}	60.0 ± 6.1^{bc}	0.0 ± 0.0	24.0 ± 4.0^{abcd}
3b	12.0 ± 2.3^{bc}	0.0 ± 0.0^{c}	60.0 ± 10.6^{bc}	0.0 ± 0.0	28.0 ± 8.3^{acd}
4b	0.0 ± 0.0^{c}	0.0 ± 0.0^{c}	68.0 ± 8.3^{c}	0.0 ± 0.0	32.0 ± 8.3^{acd}
DMSO	16.0 ± 8.3^{bc}	0.0 ± 0.0^{c}	48.0 ± 6.1^{abc}	0.0 ± 0.0	36.0 ± 10.1^{ad}

Values with different alphabets in the same column are significantly different at $p<0.05$.
SE: Standard error

At a concentration of 1ppm, 12-36% and 24-36% of adult emergence were observed in complexes and salts-treated larvae respectively (Table 9). Mortality was not observed in larvae treated with complexes and salts. However, 100% mortality was observed in larvae treated with 1ppm of the insecticide temephos (Table 9). Similar to the observed pattern in 25 and 5 ppm complex **7b**-treated larvae (Tables 7 and 8), 48% of them were still in the larval stage; the highest proportion among all the 1ppm treated mosquitoes (Table 9). The complex appears to delay development of the larvae at the various concentrations tested. Delaying the

mosquito's development at the larval stage is advantageous for vector control since this is the most vulnerable stage of its development.

Table 9

Developmental consequences of test compounds (1 ppm) on *Aedes albopictus* larvae

Compound	**Larvae**		**Pupae**		**Emerged Adults (%)**
	Alive (%)	**Dead (%)**	**Alive (%)**	**Dead (%)**	
5b	36.0 ± 10.1^{ab}	0.0 ± 0.0^{a}	28.0 ± 6.1^{a}	0.0±0.0	36.0 ± 9.2^{abd}
6b	20.0 ± 6.1^{ac}	0.0 ± 0.0^{a}	48.0 ± 8.3^{ab}	0.0±0.0	32.0 ± 6.9^{ab}
7b	48.0 ± 8.0^{b}	0.0 ± 0.0^{a}	40.0 ± 2.3^{ab}	0.0±0.0	12.0 ± 6.1^{ce}
8b	40.0 ± 2.3^{b}	0.0 ± 0.0^{a}	40.0 ± 8.0^{ab}	0.0±0.0	20.0 ± 6.1^{bc}
1b	16.0 ± 2.3^{cd}	0.0 ± 0.0^{a}	60.0 ± 10.6^{bc}	0.0±0.0	24.0 ± 8.3^{bdc}
2b	12.0 ± 6.1^{cd}	0.0 ± 0.0^{a}	52.0 ± 6.1^{bd}	0.0±0.0	36.0 ± 4.0^{ab}
3b	12.0 ± 4.0^{cd}	0.0 ± 0.0^{a}	52.0 ± 8.3^{bd}	0.0±0.0	36.0 ± 4.6^{ab}
4b	20.0 ± 4.0^{ac}	0.0 ± 0.0^{a}	44.0 ± 12.2^{acd}	0.0±0.0	36.0 ± 8.3^{ab}
DMSO	16.0 ± 4.0^{cd}	0.0 ± 0.0^{a}	40.0 ± 6.1^{acd}	0.0±0.0	44.0 ± 6.1^{a}
Temephos	0.0 ± 0.0^{e}	100.0 ± 0.0^{b}	0.0 ± 0.0^{e}	0.0±0.0	0.0 ± 0.0^{e}

Values with different alphabets in the same column are significantly different at $p<0.05$.

SE: Standard error

4. Conclusion:

A series of mononuclear–Ag(I)–NHC and binuclear–Ag(I)–NHC hexafluorophosphate complexes were synthesized by the reaction of corresponding nitrile functionalized benzimidazolium salts and characterized using various spectral and analytical techniques. According to X-ray spectra, the complex **8b** consists of an ionic structure which is of [2NHC-Ag_2-2NHC]$2PF_6$, (NHC: benzimidazol-2-ylidene) general formula. Complex **8b** exhibited high antibacterial activity towards *S. aureus* and *E. coli*, while complexes **5b**, **6b** and**7b** were moderately effective against both bacteria strains. DNA binding properties were investigated by using UV absorption spectra and viscosity measurements. All these results indicate that the complexes bind to *Aa*-DNA in an intercalative mode, by a large hypochromicity of 32 and 28% and smaller hypochromicity of 18 and 21%. The complexes displayed some degradation

effect on plasmid DNA and *Ae. albopictus* genomic DNA. The complexes, especially **8b**, were highly larvicidal and adversely affected the development of larvae into adults at the tested concentrations.

Supplementary Material

Crystallographic data for the structure in this work has been deposited at the Cambridge crystallographic data Centre, CCDC **984717.** Copies of this material can be obtained from the director, CCDC, 12 Union Road, Cambridge CB2 1EZ, UK, (fax: +44-1223-336033; e-mail: deposit@ccdc.cam.ac.uk.

Acknowledgments

R. A. Haque and M. R. Razali thank Universiti Sains Malaysia for the Research University grant 1001/PKIMIA/811346. P. O. Asekunowo thanks USM for a postdoctoral fellowship.

References

[1] K. Shalini, P.K. Sharma, N. Kuma, Der Chemica Sinica. 1 (2010) 36-47.

[2] M. Porchia, M. Pellei, M. Marinelli, F. Tisato, F. Del Bello, C. Santini, Eur. J. Med. Chem. 146 (2018) 709-746.

[3] N.A. Johnson, M.R. Southerland, W.J. Youngs, Molecules. 22 (2017) 1263-1283.

[4] M. Marinelli, C. Santini, M. Pellei, Curr. Top. Med. Chem.16 (2016) 2995-3017.

[5] H.Valdés, D. Canseco-González, J.M. German-Acacio, D. Morales-Morales, J. Organomet. Chem. 2018, DOI: 10.1016/j.jorganchem.2018.01.008.

[6] F. Gümüş, Ö. Algül, G. Eren, H. Eroğlu, N. Diril, S. Gür, A. Özkul, A. Eur. J. Med. Chem. 38 (2003) 473-480.

[7] D. Kumar Sau, R.J. Butcher, S. Chaudhuri, N. Saha, Mol. Cell. Biochem. 253 (2003) 21-29.

[8] A.T. Wan, R.A.J. Conyers, C.J. Coombs, J.P. Masterton, Clin. Chem. 37 (1991) 1683-1687.

[9] A.B.G. Lansdown, Crit. Rev. Toxicol. 37 (2007) 237-250.

[10] F. Hackenberg, G. Lally, H. Müller-Bunz, F. Paradisi, D. Quaglia, W. Streciwilk, M. Tacke, Inorg. Chim. Acta. 395 (2013) 135–144.

[11] R.A. Haque, A.W. Salman, S. Budagumpi, A.A.-A. Abdullah, Z.A. Abdul Hameed Al-Mudaris, A.M.S. Abdul Majid, Appl. Organomet. Chem. 27 (2013) 465–473.

[12] W. Streciwilk, J. Cassidy, F. Hackenberg, H. Müller-Bunz, F. Paradisi, M. Tacke, J. Organomet. Chem. 749 (2014) 88–99.

[13] H. Zetty Zulikha, R.A. Haque, S. Budagumpi, A. Abdul Majid, Inorg. Chim. Acta 411 (2014) 40–47.
[14] P.O. Asekunowo, R.A. Haque, J. Cood. Chem. 67 (2014) 3649-3663.
[15] P. O. Asekunowo, R. A. Haque, M. R. Razali, S. Budagumpi, Appl. Organomet. Chem. 3 (2015) 126-137.
[16] R.A. Haque, M.A. Iqbal, P. Asekunowo, A.M.S.A. Majid, M.B. Khadeer Ahamed, M.I. Umar, S.S. Al-Rawi, F.S.R. Al-Suede, Med. Chem. Res. 22 (2013) 4663–4676.
[17] WHO. Scientific Working Group Report on Dengue (WHO, Geneva, Switzerland, 2007).
[18] TDR/WHO. Dengue: Guidelines for Diagnosis, Treatment, Prevention and Control (TDR/WHO, Geneva, Switzerland (2009).
[19] M.G. Guzman, G. Kouri, Lancet Infect. Dis. 2 (2002) 33-42.
[20] D.J. Gubler, Comp. Immunol. Microbiol. Infect. Dis. 27 (2004) 319-330.
[21] ApexII, Bruker AXS Ltd., Madison, Wisconsin (2005).
[22] G. M. Sheldrick, Acta Crystallogr. Sect. A. 64 (2008) 112-122.
[23] L. J. Barbour, J. Supramol. Chem. 1 (2001)189-191.
[24] W.L. Drew, A.L. Barry, R. O'Toole, J.C. Sherris Appl Microbial 24 (1972) 240-247
[25] A.B. Lansdown, A. Williams, S. Chandler, S. Benfield J Wound Care 14 (2005) 155-160
[26] I. Wiegand, K. Hilpert, E.W.R. Hancock Nat Protoc 3 (2008) 163-175
[27] F.M.A. El-garj, S.W. Avicor, M.F.F. Wajidi, Z. Jaal, Asian Biomed. 9 (2015) 313-320.
[28] World Health Organization. Guidelines for laboratory and field testing of mosquito larvicides. WHO/CDS/WHOPES/GCDPP/ 2005.13. Geneva: WHO; 2005, p.69.
[29] S. Lozano-Fuentes, K. Saavedra-Rodriguez, W.C. Black IV, L. Eisen, J Am Mosq Control Assoc, 28 (2012) 59-61.
[30] S.W. Avicor, M.F.F Wajidi, E.O. Owusu, Environ Sci Pollut Res 24 (2017) 21138-21145.
[31] M.A. Abbassy, S.A.M. Abdelgaleil, R.Y.A. Rabie, Entomol Exp Appl 131 (2009) 225–232.
[32] W.S. Abbott, J. Econ. Entomol. 18 (1925) 265-267.
[33] M.E. Reichnann, S.A Rice, C.A Thomas, P. Doty, J. Am. Chem. Soc. 76 (1954) 3047-3053.
[34] J.Z. Lu, H.W. Guo, X.D. Zeng, Y.L. Zhang P. Zhao, J. Jiang, L.Q. Zang J. Inorg. Biochem. 112 (2012) 39–48.
[35] H.W. Guo, J.Z. Lu, Z.G. Ruan, Y.L. Zhang, Y.J. Liu, L.Q. Zang, J. Jiang, J.W. Huang J. Coord. Chem. 65 (2012) 191–204.
[36] J.R. Lakowicz, G. Webber, Biochem. 12 (1973) 4161–4170.
[37] J.Z. Lu, H.W. Guo, X.D. Zeng, Y.L. Zhang, P. Zhao, Jiang J, L.Q. Zang, J. Inorg. Biochem. 112 (2012) 39-48.
[38] X.W. Liao, W.J. Pan, R.W. He, H.W. Guo, P. Ying, J.Z. Lu, Chem. Biol. Drug. Des. 83 (2014) 367-378.
[39] J.L. García-Giménez, M. Gonzáles-Alvarez, M. Liu-Gonzáles, B. Macías, J. Borrás, G. Alzuet , J. Inorg. Biochem. 103 (2009) 923-934.
[40]. S. Tsiliou, L.A. Kefala, F. Perdih, I. Turel, D.P. Kessissoglou, G. Psomas, Eur. J. Med. Chem. 48 (2012) 132-142.

[41] R.A. Haque, S. Budagumpi, S.Y. Choo, M.K. Choong, B.E. Lokesh, K. Sudesh, Appl. Organomet. Chem. 26 (2012) 689-700.
[42] P.O. Asekunowo, R.A. Haque, M. Razali, S.W. Avicor, M.F. Wajidi. Appl. Organomet. Chem. 31 (2017) (7).
[43] S. B. Kalia, K. Lumba, G. Kaushal, M. Sharma, Indian J. Chem.2007, 46, 1233-1239.
[44] W. J. Geary, Coord. Chem. Rev. 7 (1971) 81-122.
[45] P. O. Asekunowo, R. A. Haque, M. R. Razali, Transit. Met. Chem. 40 **(**2015) 79-88.
[46] P. O. Asekunowo, R. A. Haque, M. R. Razali, Rev. Inorg. Chem. 37 (2017) 29-50.
[47] B. Peng, H. Chao, B. Sun, H. Li, F. Gao, L.N. Ji, J. Inorg. Biochem. 101 (2007) 404–411.
[48] P. F. Pasternack, F. J. Gibbs, J. Villatrnaca, Bio. Chem. 22 (1983) 2406-2414.
[49] M. T. Carter Rodriguez, A. J. Bard, J. Am. Chem. Soc. 111 (1989) 8901.
[50] R. Breslow I. E. Overman, J. Am. Chem. Soc. *92* (1970) 1075.
[51] S. A. Tysoe, R. J. Morgan, A. D. Baker, T. C. Strekas, *J. Phys. Chem.* **1993**, *97*, 1707.
[52] O. Sánchez, S. González, Á. R. Higuera-Padilla, Y. León, D. Coll, M. Fernández, P. Taylor, I. Urdanibia, H. R. Rangel, J. T. Ortega, W. Castro, *Polyhedron* **2016**, *110*, 14.
[53] R. A. Haque, S. Budagumpi, S. Y. Choo, M. K. Choong, B. E. Lokesh, K. Sudesh, Appl. Organomet. Chem. **2012**, *26*, 689.
[54] S.B. Aher, P.N. Muskawar, K. Thenmozhi, P.R. Bhagat, Eur. J. Med. Chem. 81 (2014) 408-419.
[55] P. Agarwala, S. Pandey, K. Mapa, S. Maiti, Biochemistry. 52 (2013)1528-1538.
[56] F. Arjmand, S. Parveen, M. Afzal, M. Shahid, J. Photochem. Photobiol. B. 114 (2012) 15-26.
[57] J.G. Liu, B.H. Ye, H. Li, L.N. Ji, R.H. Li, J.Y. Zhou, J. Inorg. Biochem. 73 (1999) 117-122.
[58] A. Wolfe, G. H. Shimer, T. Meehan, Bio. Chem. 26 **(**1987) 6392-6396.
[59] H. Ranson, J. Burhani, N. Lumjuan, W.C. Black IV. TropIKA.net 1 (2010).
[60] E.A.Temu, C. Maxwell, G. Munyekenye, A.F.V. Howard, S.Munga, S.W.Avicor, R. Poupardin, J.J. Jones, R. Allan, I. Kleinschmidt, H.Ranson. PLoS One 7 (2012) e44986.
[61] SS. Cheng, HT. Chang, ST. Chang, KH. Tsai, WJ. Chen, Bioresour Technol. 89 (2003) 99-102.
[62] J. Vontas, E. Kioulos, N. Pavlidi, E. Morou, A. della Torre, H. Ranson, Pestic. Biochem. Physiol. 104 (2012) 126-131.
[63] A. Arslan, H.R. Rathor, M.U. Mukhtar, S. Mushtaq, A. Bhatti , M. Asif, I. Arshad, J.F.Ahmad, J Vector Borne Dis. 53(2016)136-143.
[64] A. Jain, S. Saxena, AK. Rai, PN. Saxena, JV. Rao, Met Based Drugs. 6 (1999) 183-186.
[65] P.A. Castelino, P. Naik, J.P.Dasappa, R.S. Sujayraj, K.S. Chandra, K. Chaluvaiah , R. Nair , M.V.S. Kumar, G.Kalthur, S.K.Adiga, Eur J Med Chem. 84 (2014) 194-9.
[66] J.B. da Silva, D.M.Navarro, A.G. da Silva, G.K.Santos, K.A. Dutra , D.R.Moreira, M.N.Ramos, J.W.Espíndola, A.D.de Oliveira, D.J.Brondani , A.C. Leite, M.Z.Hernandes V.R.Pereira , L.F.da Rocha, M.C.de Castro , B.C. de Oliveira , Q. Lan, K.M. Merz Jr, Eur. J. Med. Chem. 100 (2015) 162-175.

[67] G. Eng, X. Song, Q. Duong, D. Strickman, J. Glass, L. May, Appl. Organomet. Chem. 17 (2003) 218-225.

HIGHLIGHTS

- New mononuclear-Ag(I)–*N*-heterocyclic carbene and binuclear–Ag(I)–*N*-heterocyclic carbene hexafluorophosphate complexes with good anti dengue potency were developed.
- Compound **5b**, **6b** and **8b** were highly active, affecting the developmental progression from the larval to the adult stage
- The most active compound, **8b** could effectively intercalate into DNA to form **8b**–DNA
- The primary in vitro assay of tested complexes against gram–positive and gram–negative bacterial strains demonstrated MICs in the range 12.5–100 μg/mL.